ROPOD

cooperative transportation of hospital beds

Paes, N.G.

Award date:
2018

ROPOD:

COOPERATIVE TRANSPORTATION OF HOSPITAL BEDS

N.G. PAES

CST 2018.006

Master's Thesis

Coach: DR. C.A. LOPEZ MARTINEZ MSC.

Supervisors: PROF. DR. H.P.J. BRUYNINCKX
DR. IR. M.J.G. VAN DE MOLENGRAFT

Committee: PROF. DR. H.P.J. BRUYNINCKX
DR. IR. M.J.G. VAN DE MOLENGRAFT
DR. IR. R. TOTH

Eindhoven University of Technology
Department of Mechanical Engineering
Control Systems Technology

Eindhoven, January 24, 2018

CONTENTS

Cooperative Transportation of Hospital Beds

N.G. Paes, C.A. Lopez-Martinez, M.J.G. van de Molengraft, H.P.J. Bruyninckx

***Abstract*—Transportation of heavy objects is one of the main causes of back pain among medical staff. Therefore, the goal of this research is to assist the medical staff with two or more robots that cooperatively transport a bed according to the commands sent by the operator. The system will have to operate safely in an environment with obstacles and limited space. The robots used in this project are omni-directional, connected to the transported object by a quasi-rigid link and with possibly unreliable communication. To analyse the system, it is modelled as a one dimensional MIMO system, where the hospital bed is defined as a varying load. A decentralized controller system is constructed which first transforms the received signal from the operator to a second order velocity reference signal, in order to have fluent movements. A velocity based low bandwidth controller and a feedforward controller are designed, such that the system is robust against the object mass variation. Due to the large dimensions of the object, detecting obstacles is only possible in a limited area. Under normal conditions, the robots communicate with each other to synchronously brake when potential collisions are detected by one or several robots. However, if the communication among robots is interrupted, a situation where some robots brake and the others try to continue is possible. Thus, the following solution is proposed, the robots with limited visibility can estimate the other robot's effort by means of an observer. Therefore, the system is transformed to a leader-follower system, where the follower applies the observed forces from the leader. The stability of the two different systems with variation in mass is analysed and guaranteed. Since the proposed solutions rely on a system model, the performance is also analysed taking into account the variations of the estimated parameters from the real ones. In order to verify the results, the algorithm is applied on the soccer robots of TechUnited when transporting a flight case which can vary in load.**

***Index Terms*—MIMO system, Cooperative Transportation, Variable mass, Observer.**

I. Introduction

Automated Guided Vehicle's (AGV's) are able to move autonomously in an environment where there can be obstacles that are not priorly known. An AGV system consists of a collection of vehicles and a central control unit, where the control unit determines the task of each vehicle. Such systems are used in a variety of industries, like manufacturing, distribution and transportation. Each application has tasks that are repetitive, follow the same route, the same routine etc. Therefore, these tasks can be performed by AGV's, which are consistent, untiring and error free [1]. However, current AGV systems use containers, boxes or carts which are customized for every AGV type, making the implementation of the AGV system more expensive. If the cargo changes in size, in shape, in weight or in pick up procedure, the AGV needs to be adjusted accordingly [2].

One of the industries where AGV systems are rarely implemented are hospitals. Large hospitals have an entire transportation network, where a large number of objects are transported daily. Moreover, moving hospital beds is a very common task and it is the cause for one of the major problems among medical staff, namely back pain [3]. Over 87% of the medical staff experiences back pain at some point in their career [4] [5]. The weight of a hospital bed ranges from 100 to 500 kilograms. The amount of force necessary to move such heavy objects ranges from 100 to 600 newton. The average pushing force a person can deliver without any risk of injuries is 225 newton [6], under the condition that it happens for a short period of time i.e. less than five seconds. Therefore, it can be stated that assistance during transportation will reduce the risk of back injuries. There are already systems available which reduces the force needed to move hospital beds, see Figure 1. However, these systems reduce the manoeuvrability

(a) StaminaLift [7] (b) Gzunda [8]

Fig. 1. Different types of existing hospital bed transporters.

of the hospital bed, contain no safety measures for obstacle collisions and are limited to moving hospital beds only. For this reason and the inability of current AGV systems to handle the diversity of objects that are transported in hospitals, the ROPOD project is started. ROPOD is an European project with two main focuses, to automate the delivery of goods within hospitals and give support during the transportation of hospital beds. The idea behind the ROPOD project is to design an AGV, called ropod, which support the people who do this work every day. In order to accomplish the transportation of hospital beds, two or more ropods will be used, which is called cooperative transportation.

The planning and coordination of a multi robot system can either be done by a centralized processing controller or by separating it among the individual controllers of the robots. A central control unit (CCU) takes all sensors and positions of each robot into account to determine the control action of the individual robots. Since each robot has wireless communication, this method is highly dependent on the performance of the communication [9]. The fact that all control is done

from one unit makes it vulnerable to complete system failures, because if this unit breaks down the entire system breaks down. The second method, where the control is performed by the individual robots, opens the possibility to make the system more robust against communication delays and system failures. If one unit breaks down, the rest could still adapt to fulfil the desired objective.

There is a lot of research done in cooperative transportation, but it is not yet used in commercial applications [10]. Cooperative transportation will provide multiple advantages for the transportation of large and heavy objects: increase in manoeuvrability due to more contact points to exert force on the load, reduced amount of force needed per robot and no adjustments of the robots needed for different sized objects. The research area is not limited to land robots only, the technique can also be applied for transportation on water [11] or for transportation through the air [12]. Multiple methods to solve the cooperative transportation problem are proposed, however each method is designed for a specific connection between robot and object. Possible connections which are proposed are, a unconstrained connection [13] [14], a partially constrained connection [9] [10] [15] or a quasi-rigid connection [16] [17]. A unconstrained connection, means that the robot is free to move with respect to the object. This system is very flexible to variations in the shape of the object. Possible methods to solve cooperative transportation using a unconstrained connection, is using potential fields [14] [18]. Under the condition of object closure, meaning that each degree of freedom of the object is constrained by the robots, the potential field approach will result in trajectory following. However, the resulting motion is non-smooth and there is no compensation for the internal force present in the system, where internal force is the force that is applied to the system by the robots in opposite direction to each other therefore does not result in any movement but in stress in the object. Another method proposed in [13], uses a centralized control scheme with the inverse Jacobian matrix to determine the desired position and velocity of the individual robots. The method requires explicit communication because of the centralized control structure. A partially constrained connection means that the robot has one degree of freedom with respect to the object. A possible method using this connection is constrained and move [9], [19], where the object is transported by applying force in the desired direction while restricting the movements in the undesired direction. The method needs at least three robots and is very dependent on communication. In [10] and [20] formation control is proposed, the system is defined as a leader follower system. The follower robot must remain at a certain distance from the leader or object, while the leader follows a reference signal, therefore no explicit communication is necessary. The connection is designed such that the effects of slip are not effecting the stability. The quasi-rigid connection is less used, because of the necessity of a coupling mechanism which might require adjustments of the load. The method proposed in [16], uses a decentralized velocity controller designed on the dynamics of the robots. Using the velocity controller decreases the internal forces present in the system. However, the method uses wired communication, which is not the case for the ROPOD project.

The proposed methods use either explicit communication or knowledge of the surroundings in order to perform path planning. In comparison with the ROPOD project, no trajectory generation is present and the communication is limited. The error in position encoder data due to slip results in the robots working against each other, therefore a compliant connection is used to limit the internal forces [9] [20] . However, the internal force present in the system by opposing forces are neglected or even used for control purposes [21], while internal forces can damage the object and cause unnecessary energy consumption. The methods take different shaped objects into account while the variation in mass is not investigated. For the ROPOD project the variation in mass is an important issue because of the variation of the hospital bed masses. The explicit necessity of communication is an critical issue for the proposed method in [13], creating a ”handicapped” mode where communication among robots is not a necessity, will provide the ROPOD project with robustness against communication failure.

Therefore, the cooperative transportation of hospital beds using the ropod is investigated in this master thesis. Two systems will be investigated, the system with full communication and the system where one ropod communication is broken. The problem definition is given in Chapter II. After which the dynamical system of the object and robots is defined and analysed, Chapter III. The control scheme present on the system and the low level control is defined in IV. Thereafter, the system where one robot is without communication is investigated, Chapter V. An experimental set up is created using the Turtles of TechUnited, the algorithm is applied on the set up and the results are analysed in Chapter VI. Ending with conclusions and recommendations for future research, Chapter VII.

II. Problem Definition

A. Problem Statement

The problem is, moving a hospital bed using multiple robots in limited spaced areas with obstacles, where the direction and velocity is controlled by an operator. The difficulty with the transportation of hospital beds is their weight and size. Using two or more robots means that the load of the object is divided among the robots. However, using multiple robots can result in robots applying force in opposing direction, resulting in internal forces. Internal forces can lead to damage to the object and unnecessary energy consumption, therefore these should be limited. The flock of robots need to do this semi-autonomously, meaning that the general guidance will be done by the user, but the robots need to prevent collisions with obstacles. During all movements of the hospital bed, the patient's comfort must be taken into account. A schematic drawing of the situation is presented in Figure 2.

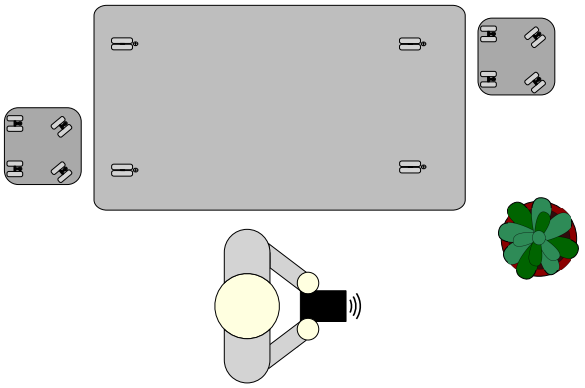

Fig. 2. A schematic drawing of the cooperative transportation problem, where the operator is controlling the object which is transported by two robots in an environment with obstacles.

B. Main Objective

Construct an algorithm whose inputs are the external commands given by the operator and as output the force commands for each robot, resulting in the movement of the hospital bed in the commanded direction.

Sub-objectives:

- Interpretation of the external commands in order to determine the necessary force magnitude and direction, exerted by each ropod.
- Obstacle collision avoidance, if the path of the ropod is obstructed by an obstacle the system needs to prevent a collision.
- Maintain comfort of the patient during transportation. Prevent sudden movements and maintain a smooth ride.
- To prevent damage to the object and unnecessary energy consumption, the internal forces present in the object should be limited
- Th algorithm should provide robustness against mass variations of hospitals beds.
- The communication between the robots and operator is wireless, thus the algorithm must be robust against loss of communication.

C. Requirements

The requirements can be formulated taking into account the objectives provided earlier. The first requirement is the maximum speed, this one should be comparable to what humans are capable of while transporting a hospital bed. On average a human walks 5 km/h (1.4 m/s), once in a hurry this can be increased to 9 km/h (2.5 m/s) [22]. Meaning, the maximum speed a human can achieve while pushing an object will be 9 km/h (2.5 m/s). Therefore, the maximum speed of the ropod will be 9 km/h (2.5 m/s), in order to achieve the same movements as a human operator. This speed must be adjustable according to the situation at hand and the standard speed will be 5 km/h (1.4 m/s). The acceleration of a human while pushing an object can be estimated by the maximum force a human can apply (225N [6]), without any risk of injury, divided by the mass of the object (not including the effects of friction). The weight of the combination of hospital bed and patient is between the 100 and 500 kg, meaning that the possible acceleration by two operators is between 0.45 and 2.25 m/s^2. While this estimation is based on the fact that both operators provide the maximum force, which in practice will not be the case, the number gives an indication of the acceleration that is achievable by the human operators. In order to maintain a smooth movement of the hospital bed and avoid patient discomfort, the jerk (m/s^3) should also be limited. Limiting the jerk will result in no sudden large accelerations or deceleration changes. No previous research has been done on the limits for acceleration and jerk during the transportation of sick people. However, a comparison can be made with elevators, although the movements are vertical, research shows that people experience accelerations between 1.3 and 1.6 m/s^2 and a jerk of 6.0 m/s^3 acceptable [23]. Hence the velocity limit will be set on 1.4 m/s, the acceleration on 1.3 m/s^2 and the jerk on 6 m/s^3.

The external commands provided by the operator need to be implemented in the desired direction. However, in case an obstacle is blocking the path, a collision should be prevented. In case of a potential collision the system needs to break without performing avoiding steering, due to the large dimensions of the object any undesired movements by the operator need to be avoided.

The final controller should be able to control the system with a variable mass between 100 and 500 kg. It is assumed that the system does not suddenly change in mass during transportation. The change in mass occurs when the system is in rest, for example the patient is removed from the hospital bed or the robots connect to a different type of bed.

III. Dynamic Model

The connection between robot and object has an effect on the dynamical behaviour of the system. Possible connections are unconstrained connection, partially constrained connection and quasi-rigid connection. In order to achieve the cooperative transportation of hospital beds, the quasi-rigid connection is used. With such a connection each robots can apply force to the object in the direction of the three degrees of freedom, therefore maintaining the omni-directionality of the object. Moreover, the robots can be located at any position around the bed, thereby minimizing the occupied space of the system. For further motivation behind the choice see Appendix A-A. In order to model the dynamics of the system, the system is modelled as a mass-spring-damper system.

A. Mass-spring-damper system

For analysis and control design, the system consisting of two robots and a relative large mass is simplified to a mass-spring-damper system. The system consisting of three dynamical systems R_1, m_{obj} and R_2, respectively robot one, object and robot two, which are interconnected by a spring-damper as representation of the quasi-rigid connection. The dynamical system of the robot is defined in three different ways, a simple mass-damping system, a state-space representation of the robot

or the frequency response date of the robot. Depending on the purpose of the model, the dynamical representation of the robot is changed. In the schematic overview presented in Figure 3, the robots are depicted as a mass-damper system. The quasi-rigid connection is represented by a spring and a damper, with stiffness k_i and damping d_i. For the simplified system it is assumed that two robots can deliver enough force to move the mass m_2 however, the system can be expanded to more robots. The two robots are able to apply forces to the

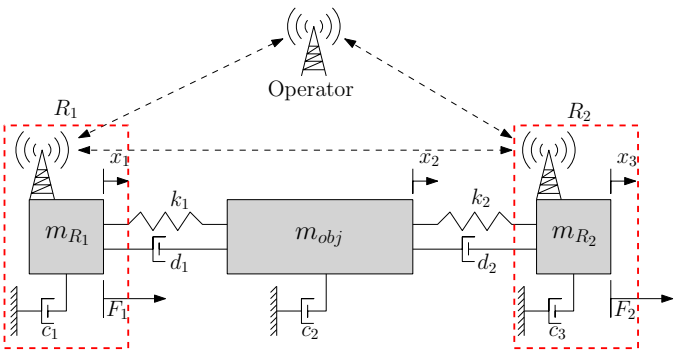

Fig. 3. Simplified mass spring damping system, where the quasi-rigid connection is defined as a spring and a damper. The robot dynamics R_1 and R_2 are depicted as mass-damper systems. The communication network between robots and operator is visualised where the network protocol is specified in Section III-B

system, which are represented by the F_1 and F_2. The system is written in state-space representation, with

$$\begin{aligned} \dot{x}(t) &= Ax(t) + Bu(t) \\ y(t) &= Cx(t) + Du(t), \end{aligned} \tag{1}$$

where $x(t) = [x_1(t), x_2(t), x_3(t), \dot{x}_1(t), \dot{x}_2(t), \dot{x}_3(t)]$, with x_i and $\dot{x}_i$ being the position and velocity of object i, see Figure 3. The output of the system is defined as the velocities of the robots R_1 and R_2. For a further elaboration of the state space representation and plant dynamics see Appendix A-B. The influence of the mass of the object on the overall dynamics of the system is visible in Figure 4, where the bode of the system is depicted for a set of different masses.

B. Communication

The communication protocol that is used for the ROPOD project is Zigbee [24]. Zigbee is a communication protocol with minimal energy consumption, which is made for simple devices. The advantage is the low latency, lower than 15 ms, however the limitation of the network is the data rate of 250 Kbps [25]. Given that the data rate is limited, the communication interval reduces the more data is sent. However, it is assumed that the communication interval is 10Hz between operator and robots. The communication network present in the mass-spring-damper system is displayed in Figure 3.

C. Internal Force

The internal force in the system is one of the aspects of the cooperative transportation algorithm that is investigated. It

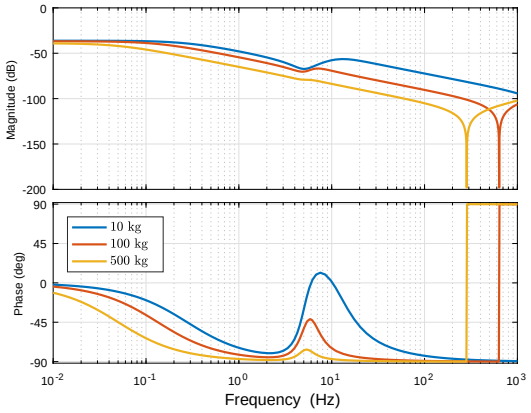

Fig. 4. The bode diagram of the mass spring damper system with state space representation of the robots included. The bode is the response from force input to velocity output of a single robot.

is the force that is present within the system which does not result in any movement. The internal force can cause damage to the object and results in unnecessary energy consumption, therefore should be avoided. The internal force in the object is present if the robots apply force in opposing directions,

$$F_{int} = \begin{cases} |F_1| + |F_2| - |F_1 + F_2|, & \textit{if } \text{sign}(F_1) \neq \text{sign}(F_2) \\ 0, & \textit{otherwise}. \end{cases} \tag{2}$$

For the three dimensional system, which is defined in Chapter IV, the internal force is also defined according to Equation (2), however F_1 and F_2 are then the forces in y-direction, see Figure 14.

IV. Control Structure

The cooperative transportation algorithm consists of two levels of control, high and low level control. A simplified version of the entire control scheme present on each robot is defined in Figure 5. The control structure is a decentralized control method, meaning that the individual robots determine on their own what forces need to be applied, the elaboration behind this choice can be found in Appendix B. The input signal of the system is provided by the operator. This reference signal can be force, position or velocity based. In order to simplify the use of the robotic assistance for the operator, the control should be easy and straight forward. The operator is used to applying force to the object in order to make it move, according to the direct force feedback felt from the bed, adjustments are made on the applied force in order to achieve the demanded movement. However, the direct force feedback will not be present if the commands are provided on an external terminal. Although there are options to implement the direct force feedback, by using for example haptic feedback [26], the adjustment of the force reference to achieve a certain movement are uncertain. Another option for the reference signal, is position based. Which means that the operator defines a position in the real world for the system to go

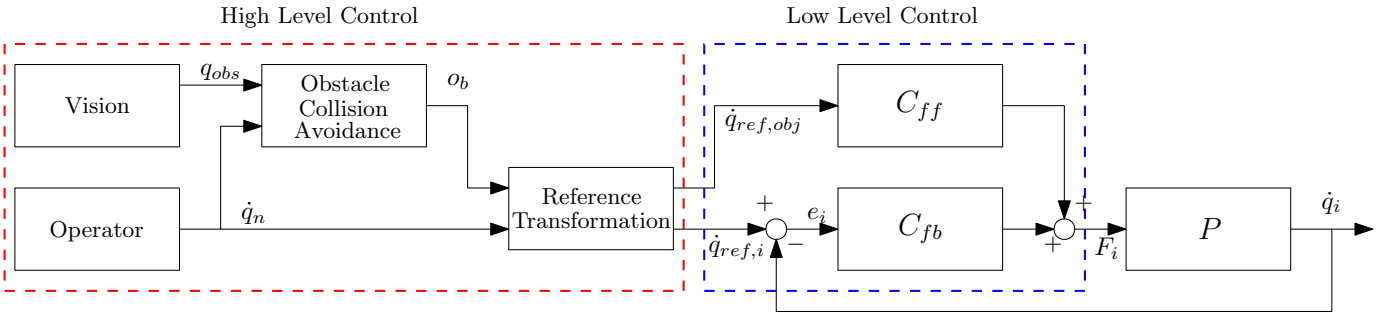

Fig. 5. The cooperative transportation control scheme present on each robot, divided into two sections high and low level control. The high level control is elaborated in Appendix C, while the low level is described in Section IV.

to. This would mean that the global position of the system needs to be known and the operator has no control over how the goal position is approached. A more straightforward way of controlling the object is the use of a velocity reference. The operator defines the velocity and direction in which the object must move. The operator gets feedback through its own observation of the system and makes adjustments accordingly. Therefore, it is chosen to use a velocity reference as signal obtained from the operator.

For the experimental set-up, the operator uses buttons as command input for the reference, therefore the nominal object velocity signal obtained from the operator is defined as $\dot{q}_n \in \{\mathbb{R}^3, [-1, 1]\}$. It is assumed that the relative distance d_r and angle ϕ to the obstacles with respect to the robot are provided with $q_{obs} = [d_r, \phi_r, R] \in \mathbb{R}^3$. At this point, it is assumed that any obstacle is defined by a circle with a radius R. However, it is possible to extend the method to different shaped obstacles. The signal q_{obs} is used for the obstacle collision avoidance to obtain $o_b \in \{\mathbb{N}^1, [0, 1]\}$, which is described in Appendix C-B. The signal o_b states whether an obstacle is blocking the current path and is generated based on the information of both robots. Therefore, the signal is dependent on the communication among the robots. The reference signal obtained from the operator $\dot{q}_n$ is transformed, as described in Appendix C-A, to a second order velocity reference $q_{ref,i} = [x_{ref,i}, y_{ref,i}, \phi_{ref,i}] \in \mathbb{R}^3$ for the each robot i. Furthermore, the signal $\dot{q}_n$ is transformed to an object velocity reference $\dot{q}_{ref,obj} \in \mathbb{R}^3$, which is necessary for the feedforward controller described in Section IV-B. The low level control, feedback C_{fb} is described in Section IV-A. The plant depicted as P is described in Chapter III. The inputs of the plant are the forces $F_i \in \mathbb{R}^3$ applied by robots $i = 1, 2, ..., n$. The output of the plant are the velocities $\dot{q}_i \in \mathbb{R}^3$ of robots $i = 1, 2, ..., n$. The error signal $e_i \in \mathbb{R}^3$ is defined as $e_i = \dot{q}_{ref,i} - \dot{q}_i$.

The feedback controller C_{fb} is designed on velocity level, because a position controller can lead to high internal forces due to position estimation drift, where a velocity controller is not effected by drift on position level.

A. Feedback Controller Design

The feedback controller must satisfy the demands of the design specifications. These design specifications are, capable of handling masses between 100 and 500 kg, an error margin of 15% of the reference signal and an over damped system to prevent osculating behaviour. Two different feedback controllers are designed, because of the similarities of the behaviour of the robot in the x and y axis the controllers are the same while the controller for the rotation is designed separately. For the x and y the plants behaviour is depicted in Figure 4. The design of the controller is taking the desired performance and stability margins for variable mass between 100 and 500 kg into account. The resulting controller is,

$$C_{fb,xy} = \frac{520}{0.03979s + 1} \tag{3}$$

consisting of a gain of 520 and a low pass filter of 4 hz. Due to the zero phase at low frequencies, the resulting reference tracking will contain a constant error. However, adding an integrator to the controller to counteract this effect, will transform the velocity controller into a position controller and is therefore left out. The gain of 520 is set to this particular value in order to achieve the 15% error margin. The low pass filter is included to decrease the effect of the high frequencies and to increase the damping of the system. By using a step function as reference signal on the closed-loop system with the designed controller the performance can be determined, see Figure 6a, where it is assumed that two robots are applying force. Furthermore, the nyquist diagram of the system is depicted in Figure 6b, where the frequency response data (FRD) of the turtle is used to represent R_1 and R_2 in Figure 3.

It is clear from the response to a step function as input, that the performance of the system is decreasing the larger the mass. However, both the criteria of a 15% error margin and robustness against the uncertain mass are met. Furthermore, from the step response it can be stated that the system is over damped. An over damped system has a more fluent movement which is required for the comfort of the patient, however it will result in a slow system. Based on the Nyquist diagram, where no encirclements of the unstable minus one point are present

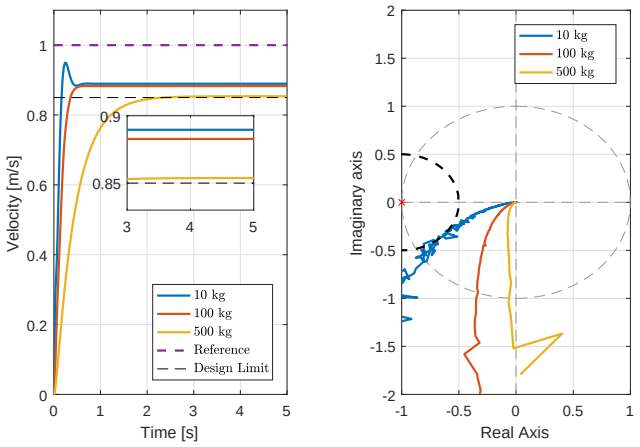

(a) Velocity step response based on state space representation presented in Section III-A.

(b) Nyquist diagram based on SISO open-loop system with FRD of the turtle for representation of the robots.

Fig. 6. The step response and nyquist diagram of the variable mass system, in order to visualise the performance and stability of the one dimensional case.

and the fact that the system contains only negative open-loop zeros and a pole at zero, the designed feedback controller C_{fb} is guaranteed stable for the one dimensional case. However, the system is a multi-input-multi-output system, therefore a more elaborate stability analysis can be found in Appendix D-A.

In order to design the controller for the rotational direction of the robot, the inertia of the entire system needs to be known. The inertia of the system is dependent on the dimensions, the mass and its distribution and rotation axis. An estimation of the inertia at the centre of the object is provided in Appendix A-C, where it is assumed that the mass is equally distributed and the system consists of rectangular shaped objects. The rotation of the robots is achieved by its own rotational controller and the translation controller $C_{fb,xy}$ of the second robot. Resulting in the fact that the performance of the rotation of the robot is dependent on both the design of the rotation and translation controllers. The rotation controller is designed on the lowest possible inertia of the system, which is the system without additional mass. The resulting controller is,

$$C_{fb,\phi} = \frac{40}{0.03979s + 1} \tag{4}$$

which has a gain of 40 and a low-pass filter of 4 Hz. Due to the large dimensions of the object, the rotation around the robot is resulting in a large translation of the other robot. This translation is controlled by $C_{fb,xy}$ and the resulting momentum of this translation is, due to the dimensions, greater than the control input generated by the controller $C_{fb,\phi}$. For movements around the centre of the object, similar conclusions can be made because this movement is controlled by the translation controllers of the two robots. Therefore, it can be concluded that the performance for rotations around the object are dependent on the design of $C_{fb,xy}$. The stability of the three dimensional system with the presented controllers $C_{fb,xy}$ and $C_{fb,\phi}$ is analysed in Appendix D-B.

B. Feedforward Controller Design

The feedforward controller is implemented in order to improve the performance of the system. A perfect feedforward controller would be the inverse of the plant P, however this plant is not fully known. From Figure 4, it can be concluded that because of the large mass of the object, the dynamics of the robot have less of an influence on the overall dynamics of the system, especially at low frequencies. Therefore it is assumed that at those frequencies the system can be approximated with a first order single mass-damper system. The plant used for the feedforward controller has the structure

$$P_{FF} = \frac{1}{m_t s + d_t}, \tag{5}$$

where m_t is the total mass of the system and d_t is the total damping of the system. The parameters are based on estimated parameters of the system, with as lower bound the lowest mass of the object 100 kg. Furthermore, the Coulomb friction is compensated with a extended two dimensional friction model. For the model it is defined that the friction in x-direction is equal to $F_{r,x}$ and the y-direction is equal to $F_{r,y}$. In order to prevent that the friction is overcompensated while moving in both x and y-direction, the ratio between the absolute velocity v_{abs} and the velocity v_i in the direction i is used to determine the amount of each friction force $F_{r,i}$. The two dimensional model is extended to a three dimensional, using

$$v_{abs} = \sqrt{v_x^2 + v_y^2 + v_\phi^2}. \tag{6}$$

The amount of friction in each direction is determined using $\frac{v_i}{v_{abs}} F_{r,i}$. The resulting model is a simple three dimensional compensation of the friction with a variable friction in each direction. The goal of the model is to compensate a large proportion of the friction however, perfect tracking is not necessary. Therefore, the simple model is not further extended. The performance of the resulting control scheme is investigated on the experimental set-up, see Section VI-B and Appendix F-A.

V. Leader-Follower system

One of the sensitive aspects of the system is the communication among robots and operator. If the communication among robots fails, the robots can no longer communicate if a obstacle is blocking the path. Resulting in one robot trying to follow the reference while the other brakes, meaning a build up of internal force and a possible collision with the obstacle. Moreover, if the communication on one robot fully breaks down, this robot does no longer receive a reference signal and is therefore unable to be controlled. In situations where this happens the situation might be that the load is blocking the corridor and therefore needs to be removed. A possible solution for such situations, is to switch to a leader-follower system, as proposed in [10] [20]. However, these methods use vision information in order to determine the movements of the

leader, while the vision of the ropod in the direction of the leader will possibly be blocked by the hospital bed. Using an Observer, as proposed in [27], the robot is able to estimate the forces applied on the system based on its own movements. The control structure of the non-communicating robot is depicted in Figure 7.

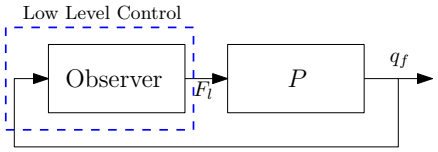

Fig. 7. The schematic representation of the control loop present on the follower robot, where F_f is the input applied by the follower robot and F_l is the estimation of the forces of the leader robot.

The observer is defined in Section V-A. The observer functions as feedback loop, due to the fact that the forces applied by the follower needs to be the same as the forces of the leader in order to achieve the desired motion. The control structure of the leader robot has a similar structure as visible in Figure 5, except for an additional force signal elaborated in Section V-B. The stability of the entire system with observer is analysed in Section V-C

A. Observer

An observer uses the inverse of the plant to reconstruct the forces applied to the system [27]. However, the plant is not known, therefore an estimation of the plant is necessary, a possible method to obtain the mass and inertia of the system is presented in Appendix E. The structure of the observer present on the follower robot is visible in Figure 8. The position x_f

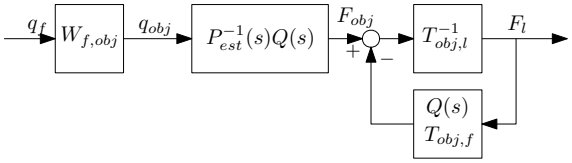

Fig. 8. The schematic representation of the observer present on the follower robot, where q_f is the position of the robot, q_{obj} is the position of the object, F_{obj} is the total force applied on the object and F_l is an estimation of the applied force by the leader robot.

of the robot is transformed using $W_{f,obj}$ to the position of the object q_{obj}, based on the offset of the robot with respect to the object, see Figure 9.

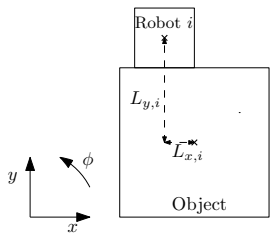

Fig. 9. The position of the robot with respect to the object, where index i is robot i.

The P_{est} is an estimation of the plant P. The estimation of the plant is based on

$$P_{est}(s) = \frac{1}{m_t s^2 + d_t s}, \tag{7}$$

where m_t is the mass and d_t is the damping of the robots and object combined. As for the feedforward signal in Section IV-B, it is assumed that the dynamics of the total system at low frequencies can be modelled with this formulation. Taking the inverse of the $P_{est}(s)$ would result in a non-causal system, therefore it is multiplied with a second order low-pass filter

$$Q(s) = \frac{g_{dis}^2}{s^2 + 2g_{dis} + g_{dis}^2} \tag{8}$$

where $g_{dis} = 2\pi f_{cut}$ with f_{cut} the cut-of frequency. The result is a filtered estimation of the total force F_{obj} applied on the system. The forces applied by the follower are transformed to the centre of the object with $T_{obj,f}$. For simplification of the transformation it is assumed that $L_{x,f} = 0$. The resulting transformation is achieved with,

$$T_{obj,f} = \begin{bmatrix} 1 & 0 & \frac{1}{L_{y,i}} \\ 0 & 1 & 0 \\ -L_{y,i} & 0 & 1 \end{bmatrix}. \tag{9}$$

where $L_{y,i} = L_{y,f}$. The resulting force is subtracted from F_{obj} in order to determine the forces applied by the leader robot F_l. The transformation of the forces is realised with the inverse of (9) where $L_{y,i} = L_{y,l}$. The result is an estimation of the forces applied by the leader robot at the position of the leader robot. Until now it was assumed for the observer that the friction in the model is only consisting of damping, however the effects of Coulomb friction can be noticed in the performance of the observer. Therefore, additional Coulomb friction is included in the plant estimation, using the method as proposed in Section IV-B.

Problems arise for movements in the x-direction. The robots are positioned with $L_y \neq 0$, therefore a force applied in x-direction for the robots results in a momentum in the centre of the object mass. Under the normal conditions where there is communication this momentum is counteracted by the other robot. But, in the situation where there is no communication the leader robot will make the object, and therefore the robots as well, rotate and translate instead of only translating. The estimation of the forces by the follower are comparable to the results in the y-direction. However, the resulting movement contains a rotation of the object. To counteract the initial rotation and additional force is introduced, which is presented in the next section.

Another problem is that the movement in ϕ-direction is no longer possible. A movement in ϕ-direction is achieved by a force applied in x-direction by the leader robot, which is similar to the movement in x-direction. And due to the fact that the forces applied by the leader robot are directly applied by the follower robot, the resulting motion will be a translation in x. Therefore, the rotational motion will require a different approach, however this will not be covered in this research.

B. Rotational Movement Compensation

An additional force signal is introduced to counteract the rotation of the object which is caused by the momentum generated by the leader robot. The additional force signal is based on human like behaviour. Take the situation depicted in Figure 10, where two persons transport a beam and person one determines in which direction the object must move, while person two is unable to see person one and determines its applied force on the movement of the object. Person one

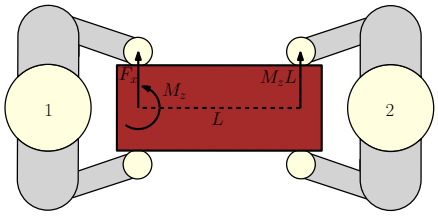

Fig. 10. A situation where two humans transport an object, where person one steers and person two is unable to see person one. Person one applies an translation force F_x in order to achieve the translation in x-direction and a rotational force M_z in order to prevent the rotational movement of the object. This initial force M_z is maintained until person two is moving in the correct direction with the same velocity as person one.

applies two forces, F_x in order to move in the direction of the force and an additional rotational force M_z which is the force person two should apply times the length of the object. This additional force is based on the amount of force person two is applying. The result is that the object is moved in the demanded direction and the additional force M_z is decreased till person two is applying the necessary force. This situation is similar to the situation of the two robots moving an object. The additional rotational force M_z is therefore applied by the leader robot. An observer present on the leader will determine the amount of force measured by the follower. The design of the observer is similar as the observer present on the follower robot. The additional force M_z is determined according to

$$M_z = 2L_y(F_{x,l} - F_{x,f}), \tag{10}$$

where L_y is the distance between the robot and the centre of the object, $F_{x,f}$ is the estimated force applied by the follower robot obtained from the observer. The force $F_{x,l}$, is the force signal applied by the leader robot. The momentum M_z goes to zero when the follower robot is applying the necessary force $(F_{x,f} = F_{x,l})$ to achieve the desired motion. The next step is the stability analysis of the non-communicative system.

C. Stability

The stability of the leader-follower system is analysed by considering the input-output relation of the leader robot. The follower input-output are directly depending on the input of the leader robot, therefore this input-output relation influences the leaders input-output. Furthermore, it is assumed that the overall dynamics of the plant at low frequencies can be approximate with a mass-damper system. The resulting control scheme is visible in Figure 11. Two control loops are visible, the leader robot and the follower robot. The reference

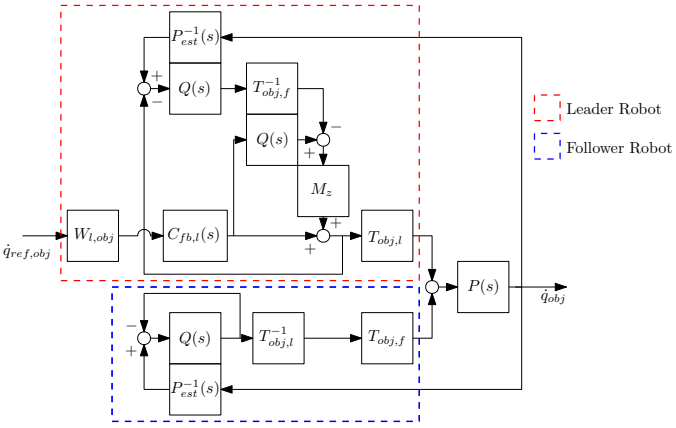

Fig. 11. Schematic representation of the three dimensional leader-follower system, which is simplified to a mass-damper system where the low level control of the robots is controlling the system.

signal $\dot{q}_{ref,obj}$ is first transformed using $W_{l,obj}$, as defined in (20), to the position of the leader robot. After which the feedback controller $C_{fb,l}$ generates the forces necessary for the movement. Using the inverse of the estimated plant P_{est} and subtracting the applied forces of the leader robot, provides the estimated forces applied by the follower robot. Comparing them to the necessary force generated by the controller $C_{fb,l}$, provides the additional force to compensate for the error. This force is transformed with M_z to the necessary torque. The control loop present on the follower robot, is the observer consisting of P_{est}^{-1}, Q and transformation $T_{obj,l}^{-1}$ to estimate the forces applied by the leader robot, neglecting the rotational force. The applied forces of each loop, are transformed to the position of the object using $T_{obj,i}$ as in (9). The combined forces of robot 1 and 2 are applied on the mass damper system.

In order to verify the stability of the three dimensional case, a factorized Nyquist test [28] is performed. With the factorized Nyquist test, the stability of the diagonal plant and the stability of the off-diagonal terms, which is the interaction, guarantees the stability of the entire system. The sensitivity S of the system is written as

$$\underbrace{(I + PC)^{-1}}_{=S} = \underbrace{\left(I + \tilde{P}C\right)^{-1}}_{=\tilde{S}} \underbrace{\left(I + E\tilde{T}\right)^{-1}}_{\text{interaction}}, \tag{11}$$

where,

$$\begin{aligned} \tilde{P} &= \text{diag}(p_{ij}) \\ E &= \left(P - \tilde{P}\right)\tilde{P}^{-1} \\ \tilde{T} &= \text{diag}\left(\frac{p_{ij}c_{ij}}{1 + p_{ij}c_{ij}}\right) \end{aligned} \tag{12}$$

with p_{ij} and c_{ij} being the (i,j) element of P and C respectively. The criteria of stability are

- $\tilde{S}$ is stable if $det\left(I + \tilde{P}C\right)$ has no encirclements of the the origin as s traverses Nyquist D-contour.

- $\left(I + E\tilde{T}\right)$ is stable if $\bar{\sigma}\left(\tilde{T}(j\omega)\right) < \mu_{\tilde{T}}^{-1}\left(E(j\omega)\right), \forall\omega$, where $\mu_{\tilde{T}}(E)$ is the structured singular value (SSV) of E with respect tot $\tilde{T}$ computed according to [28].

Due to the fact that a non-zero reference for the rotational movement cannot be controlled by the current approach, the input of the system is defined as $\dot{q}_{ref} = [\dot{x}_{ref}, \dot{y}_{ref}]$. The movement in x however influences the movement in the ϕ direction, therefore the output is defined as $\dot{q}_{obj} = \left[\dot{x}_{obj}, \dot{y}_{obj}, \dot{\phi}_{obj}\right]$. Therefore, the diagonal system consists of x and y, while the off-diagonal system has ϕ included. Since the stability will be dependent on the accuracy of the estimated plant, the stability analysis is performed for the cases where the plant is under- and overestimated, resulting in a variable sensitivity S_Δ where subscript Δ represents the variation. The parameters that are estimated are the mass and damping in x and y, although they are presumed to be similar, and the inertia and damping of the ϕ direction. Because of the large variation range of the mass of the object, the analysis is performed for the minimal and maximal of the mass range separately. The parameters of the system are visible in Table III. The results from the factorized Nyquist of the system with mass 100 kg are visible in Figure 12. The results from the system with object mass 500 kg is visible in Figure 13.

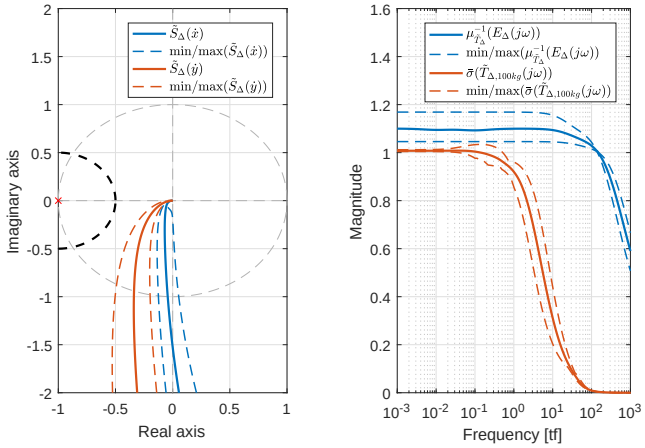

(a) The first criteria. (b) The second criteria.

Fig. 12. For the factorized Nyquist test, the Nyquist diagram and SSV of the open-loop system of x and y with object mass 100 kg are visualised, with the variation due to the error in the estimation of the plant visualised with the dashed line.

If the maximum error in the estimation of the plant is set to 30%, the resulting system is stable. This can be concluded from the results obtained from the factorized Nyquist test. The uncertainty of the system due to the fact that the analysis is based on the simplified mass-damper system, instead of the real system, is not included in the analysis. However, the resulting analysis provides a indication of the stability of the real system.

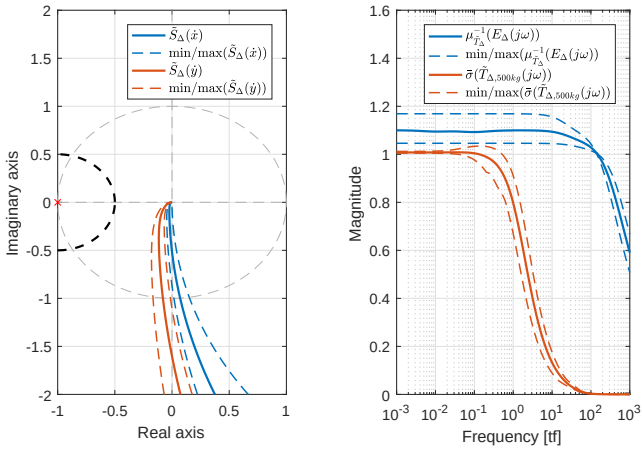

(a) The first criteria. (b) The second criteria.

Fig. 13. For the factorized Nyquist test, the Nyquist diagram and SSV of the open-loop system of x and y with object mass 500 kg are visualised, with the variation due to the error in the estimation of the plant visualised with the dashed line.

VI. Experimental Results

In order to verify the performance of the cooperative transportation algorithm, it is applied on an experimental set-up. The set-up consisting of two robots and an object is described in Section VI-A. The internal force of the communicative system is analysed, in Section VI-B, a more elaborate examination of the performance can be found in Appendix F-A. The performance of the observer based system is analysed in Section VI-C.

A. Experimental Set-up

The experimental set-up consists of two robots and one flight case. Because the Ropod is still under construction, the soccer robots of TechUnited are used, which are called Turtles. The Turtle has three omni-wheels positioned in a triangular shape, making the robot omni-directional. Its movement is measured with encoders on wheel basis, with a sample rate of 1000 Hz. The camera located at the top determines its position on the field and the obstacles in its surroundings. The control software is implemented in a Simulink environment with a sample frequency of 1000 Hz. The communication among the turtles happens via the WIFI network, however, the software is modified to emulate similar constraints as of the Zigbee network. The mass, damping and friction parameters of the turtle are experimentally determined.

The object that is transported is a flight case, which weighs 12 kilograms and is omni-directional. The weight of the object can be varied using additional load. The quasi-rigid link is created using straps. The dimensions of the object are 0.6 by 0.6 meters. The set-up is displayed in Figure 14.

B. Internal Force of Communicative System

The internal force of the system should be as minimal as possible to prevent damage and unnecessary energy consump-

Fig. 14. The experimental set up used for the validation of the cooperative transportation of objects.

tion, therefore the internal force of the communicative system is analysed. A more elaborate performance analysis of the communicative system can be found in Appendix F-A. The internal force, as defined in Section III-C, is present in the y-direction of the set-up, see Figure 14. The system is actuated in x and y-direction separately in order to determine the internal forces in the system for the two separate movements. The reference signal provided for the system is presented in Figure 15a. The resulting intern force is based on the input signal of the robot, which is assumed to be equal to the force applied by the robot. This assumption is based on the transition from input signal to wheel output. The internal forces present in the system during the movement in x-direction and y-direction are visible in Figure 15b.

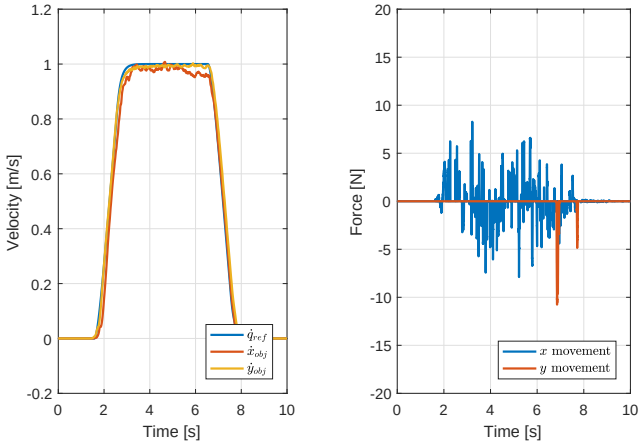

(a) The reference signal tracking in the x and y-direction

(b) The internal forces present in the system

Fig. 15. The reference tracking and internal force during the motion in x and y-direction of the communicative.

The resulting internal force in x-direction is caused by the amplification of the error signal, where the error signal contains sensor noise. Therefore the internal force in this direction is dependent on the noise of the sensors and the magnitude of the controller. Resulting in a trade-off between performance and internal force. For the y-direction, the internal force is caused by the communication delay of the system. Due to the communication delay, the two robots do not receive their signal at the same time step, resulting in one robot lacking behind. In situations when the force switches from positive to negative, the delay will result in internal force. The time period that internal forces are present, are dependent on the delay. The situation where an obstacle is blocking the path, the information is sent from one robot to the other meaning that the signal will be delayed. However, the resulting internal forces are similar to the internal forces visible in Figure 15b.

C. Performance Leader-Follower System

The performance of the leader-follower system is based on the accuracy of the estimated plant. The parameters of the experiment set-up are obtained based on experimental results. Due to the inability of the current control scheme to perform a rotational movement, only the performance in the x and y-direction is analysed. The reference signal used for the experiment, is similar to the one provided in Figure 15a, with the constant velocity lowered to 0.5 m/s and extended to 10 seconds. The resulting performance of the system in y is visible in Figure 16, where the velocity and error signal are filtered forwards and backwards in time with a 5 hz low pass filter in order to have a noise in the signal. The reference tracking in y-direction is achieved with limited error in all three axis. The delay of the follower is caused by the low pass filtering, which is also the cause for the internal force visible in Figure 16d. Furthermore, because of the static friction, the follower robot does not measure any force applied by the leader robot if the force of the leader robot is not greater than the static friction, see Figure 16c.

The performance in the x-direction is visible in Figure 17. It is clear that the performance in x-direction is lower to the performance in y-direction, which is caused by the fact that the applied force results in a rotation. The rotation as a result of the delayed observer is visible in the error signal in Figure 17b, where it can also be seen that the rotation is partially compensated after the initial movement. The estimation of the leader force by the follower robot is delayed but in steady state the result is close to the real force. The internal forces during the x movement are comparable to the communicative systems internal force, for the y movement it is significantly lower. Meaning that adding an observer to the communicative system could potentially decrease the internal forces. The additional force presented in Section V-B is visible in Figure 17, due to the delayed response of the follower robot during the initial acceleration, the additional rotation force partly compensates the rotation velocity. However, as soon as the follower starts moving the force decreases because the force applied by the follower robot gets close to the force applied by the leader. The resulting rotational movement is visible in Figure 18, where the xy movement is visualised. Because of the initial rotational movement, the entire movement deviates from the initial x axis.

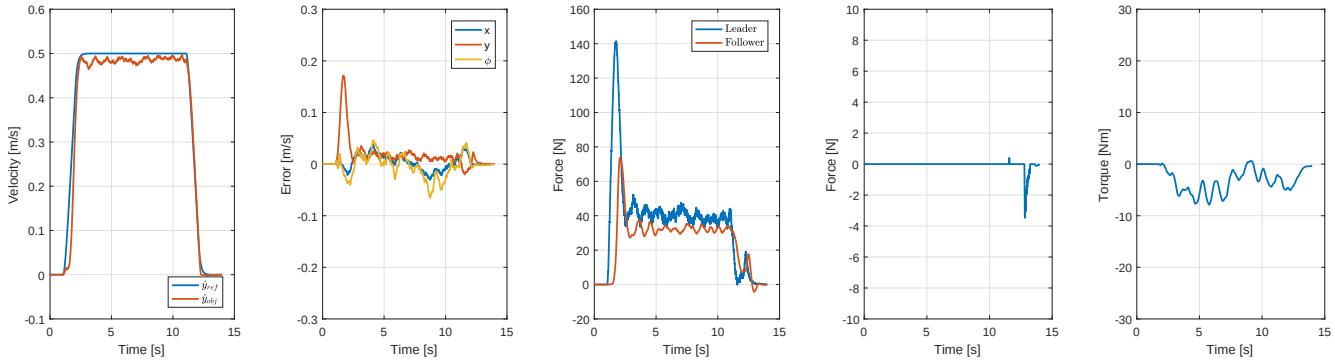

(a) Achieved Velocity versus reference signal (b) The error in the three degrees of freedom (c) Force input of the robots (d) The internal force of the system (e) The rotation compensation torque

Fig. 16. The performance of the observer based system, for a movement in the y-direction.

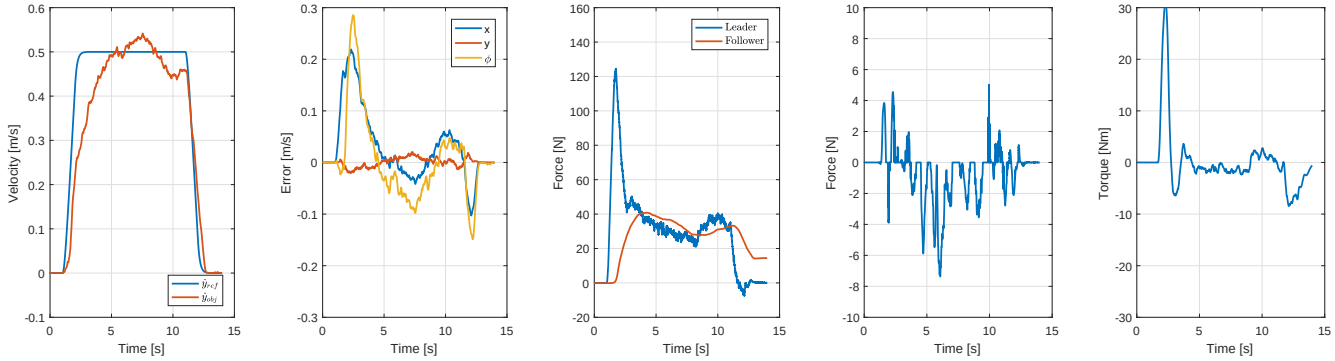

(a) Achieved Velocity versus reference signal (b) The error in the three degrees of freedom (c) Force input of the robots (d) The internal force of the system (e) The rotation compensation torque

Fig. 17. The performance of the observer based system, for a movement in the x-direction.

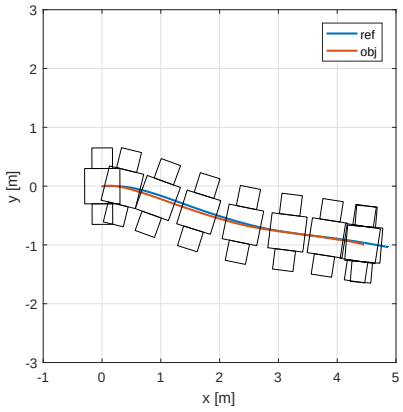

Fig. 18. The xy plot of the resulting movement for a reference in x. The reference x is local therefore the reference adjusts according to the rotation of the robots.

VII. Conclusions and Recommendations

A. Conclusion

In order to reduce the change of back injuries among the medical staff caused by the transportation of hospital beds, one of the goals of the ROPOD project is to use multiple robots for the transportation. The collaboration between multiple robots to achieve transportation is called cooperative transportation. Existing methods use unconstrained connections between object and robot or wired communication. Therefore, this project focused on the transportation with quasi-rigid connection and unreliable wireless communication. Two methods are proposed for a system with communication and a method where one robots communication is broken. The communicating system uses a decentralized control scheme, where the reference is adjusted and obstacle collisions are prevented. The low level control consists of a velocity controller which is robust against the mass range of the hospital beds. The resulting reference tracking is well within the demanded 15% error range. Furthermore, the stability of the system for the variation in mass within the predefined range is guaranteed. From the experimental results, it can be concluded that the internal force

present in the system are limited. By limiting the acceleration and jerk of the received reference from the operator, the resulting motion of the hospital is made more comfortable.

A leader-follower system is introduced to control the system in case the communication of one robot malfunctions. The system uses an observer to estimate the forces applied by the leader robot. The estimated forces are applied by the follower robot in order to achieve the cooperative transportation. Based on the observations made during experiments, where motions in the x-direction resulted in a rotational motion instead of a motion in only x-direction, an rotational movement compensation force is introduced. The compensation force is applied by the leader robot to compensate for the delayed response of the follower robot. The down side of the resulting system is the inability to rotate around the centre of the object, due to the similarities of the force applied by leader robot for x and ϕ motions, the follower robot is unable to make a distinction. However, a possibility is to determine its direction in x based on the initial torque applied by the robot, making it possible to rotate but not possible to switch during a movement. From the stability analysis, it can be concluded that the system will be stable if the estimated plant has a maximum error of 30% in the estimation of the mass and damping of the system, in comparison with the real plant. The experimental results show, that for movements in the y-direction the performance is comparable to the communicative system. The movements in the x-direction still result in undesired rotations, however the resulting rotation is caused by friction and the delay of the observer system, such effect is partially compensated with the with the proposed rotation force compensation.

B. Recommendations

For future work in cooperative transportation within the hospital environment, additional safety measures should be implemented. For the obstacle avoidance it is assumed that all obstacles can be represented with a circular shape, however this will not be the case. Therefore, the obstacle collision detection must be extended to variable shaped objects and include the recognition of walls. With the knowledge of the wall, the system might be able to follow the wall, thereby increasing the user friendliness of the system. An issue that is experienced during the experimental investigations is the effects of the miss-alignment of the robots, this results in undesired drift. If the position of the robot with respect to the bed, is not correctly known, the applied force does not result in the desired motion. Therefore, the systems needs to be made robust against miss-alignment of the robots.

For the leader-follower system it is now assumed that at least one robot receives the reference signal, therefore the system will not perform if no communication is present. An solution for this might be extending the observer to both robots, thereby making the robots estimate the applied force of the operator. However, a distinction needs to be made between the applied force by the robot and the force applied by the operator. Without the distinction, the robots will actuated each others input and while the operator is still applying force, the force of the robots will keep increasing which results in a unstable system.

Another option for the prevention of the rotation as a result of the delayed follower, is instead of estimating force of the leader robot, follow the velocity of the leader robot. Since the quasi-rigid connection its assumed that the velocity of the leader robot can be estimated based on the velocity of the follower robot. The estimated velocity will then be used as reference signal for the follower robot. For the movement in x-direction this solution might solve the delayed reaction of the follower robot. However, the down side is that the movement in y-direction will result in the leader robot doing all the work, because the reference signal for the follower robot is exactly its own velocity. Thus, one might implement a combination of this recommendation in x-direction and the presented approach in the y-direction.

REFERENCES

[1] I. F. A. Vis. Survey of research in the design and control of automated guided vehicle systems. *European Journal of Operational Research*, 170(3):677–709, 2006. 1

[2] Günter Ullrich. *Automated Guided Vehicle Systems: A Primer with Practical Applications*. Springer Berlin Heidelberg, Berlin, Heidelberg, 2nd ed. edition, 2015. 1

[3] Kyung Ja June and Sung Hyun Cho. Low back pain and work-related factors among nurses in intensive care units. *Journal of Clinical Nursing*, 20(3-4):479–487, 2011. 1

[4] Bureau Of Labor Statistics. Lost-worktime injuries and illnesses: Charatieristics and resutling days away from work. *English Journal*, 344(9):673–675, 2005. 1

[5] A. Karahan and N. Bayraktar. Determination of the usage of body mechanics in clinical settings and the occurrence of low back pain in nurses. *International Journal of Nursing Studies*, 41(1):67–75, 2004. 1

[6] The Eastman Kodak Company. *Kodak ' s Ergonomic Design Kodak ' s Ergonomic Design for*. John Wiley & Sons, Inc., Corporate Clearance, Eastman Kodak Com- pany, 1999 Lake Avenue, Rochester, NY, 2de edition, 2004. 1, 3

[7] Staminalift. StaminaLift TS5000 Transfer System. [Online]. Available: http://staminalift .com/transfer_solutions/ts5000_transfer_system/. [Accessed: 20-feb-2017]. 1

[8] GZUNDA Bed Mover. [Online]. Available: http://www.arjohuntleigh.com.au/products/medical-beds/gzunda-gz10-bed-mover/specifications/. [Accessed: 22-feb-2017]. 1

[9] Aram Zaerpoora, Majid Nili Ahmadabadia, Mohammad R. Barunia, and Z. D. Wang. Distributed object transportation on a desired path based on Constrain and Move strategy. *Robotics and Autonomous Systems*, 50(2-3):115–128, 2005. 1, 2

[10] Xin Yang, Keigo Watanabe, Kiyotaka Izumi, and Kazuo Kiguchi. A decentralized control system for cooperative transportation by multiple non-holonomic mobile robots. *International Journal of Control*, 77(10):949–963, 2004. 2, 6

[11] J. Shao, L. Wang, and J. Yu. Development of an artificial fish-like robot and its application in cooperative transportation. *Control Engineering Practice*, 16(5):569–584, 2008. 2

[12] Jonathan Fink, Nathan Michael, Soonkyum Kim, and Vijay Kumar. Planning and control for cooperative manipulation and transportation with aerial robots. *Springer Tracts in Advanced Robotics*, 70(STAR):643–659, 2011. 2

[13] I Mas and C Kitts. Object manipulation using cooperative mobile multi-robot systems. *Proceedings of the World Congress on Engineering ...*, I, 2012. 2

[14] Peng Song and Vijay Kumar. A potential field based approach to multi-robot manipulation. *Proceedings 2002 IEEE International Conference on Robotics and Automation (Cat. No.02CH37292)*, (May):1217–1222, 2002. 2

[15] Bruce Donald, Larry Gariepy, and Daniela Rus. Distributed manipulation of multiple objects using ropes. *Proceedings-IEEE International Conference on Robotics and Automation*, 1(April):450–457, 2000. 2

[16] B. Stouten and A. J. de Graaf. Cooperative transportation of a large object - development of an industrial application. *IEEE International Conference on Robotics and Automation, 2004. Proceedings. ICRA '04. 2004*, 3(April):2450–2455 Vol.3, 2004. 2

[17] Taher Hekmatfar, Ellips Masehian, and Seyed Javad Mousavi. Cooperative object transportation by multiple mobile manipulators through a hierarchical planning architecture. *2014 2nd RSI/ISM International Conference on Robotics and Mechatronics, ICRoM 2014*, pages 503–508, 2014. 2

[18] V. Kumar. Object closure and manipulation by multiple cooperating mobile robots. *Proceedings 2002 IEEE International Conference on Robotics and Automation*, 2002(May):394–399, 2002. 2

[19] Z. Wang, M.N. Admadabadi, E. Nakano, and T. Takahashi. A multiple robot system for cooperative object transportation with various requirements on task performing. *Proceedings 1999 IEEE International Conference on Robotics and Automation*, (May):1226–1233, 1999. 2

[20] Toni Machado and Tiago Malheiro. Multi-constrained joint transportation tasks by teams of autonomous mobile robots using a dynamical systems approach *. *2016 IEEE International Conference on Robotics and Automation (ICRA) Stockholm, Sweden, May 16-21, 2016*, pages 3111–3117, 2016. 2, 6

[21] Z. Wang, Y. Takano, Y. Hirata, and K. Kosuge. A pushing leader based decentralized control method for cooperative object transportation. *2004 IEEE/RSJ International Conference on Intelligent Robots and Systems (IROS) (IEEE Cat. No.04CH37566)*, 1:1035–1040, 2004. 2

[22] Raymond C Browning, Emily A Baker, Jessica A Herron, and Rodger Kram. Effects of obesity and sex on the energetic cost and preferred speed of walking. *Journal of applied physiology (Bethesda, Md. : 1985)*, 100(2):390–8, 2006. 3

[23] R.E. Howkins. Elevator Ride Qualtiy - The Human Experience. *The original*, (1), jan 2007. 3

[24] Zigbee Alliance. [Online]. http://www.zigbee.org. [Accessed: 13-Nov-2017]. 4

[25] ZigBee vs Bluetooth and Bluetooth Smart. [Online].https://www.allaboutcircuits.com/technical-articles/zigbee-vs-bluetooth-and-bluetooth-smart/.[Accessed: 13-Nov-2017]. 4

[26] D. Richert and C.J.B. Macnab. Direct adaptive force feedback for haptic control with time delay. *2009 IEEE Toronto International Conference Science and Technology for Humanity (TIC-STH)*, pages 893–897, 2009. 4

[27] K S Eom, I H Suh, W K Chung, and S R Oh. Disturbance observer based force control of robot manipulator without force sensor. *Proceedings 1998 IEEE International Conference on Robotics and Automation Cat No98CH36146*, 4(May):3012–3017, 1998. 7

[28] Sigurd. Skogestad and Ian. Postlethwaite. *Multivariable feedback control : analysis and design*. John Wiley, 2005. 8, 9

[29] V. Adams and A. Askenazi. *Building Better Products with Finite Elements*. OnWOrd Press, Santa Fe, 1 edition, 1999. 15

[30] J.C. Robert H. *Dynamics of Physical Systems*. Dover Publications, Dover, 2012. 20

[31] Frank Boeren, Tom Oomen, and Maarten Steinbuch. Iterative motion feedforward tuning: A data-driven approach based on instrumental variable identification. *Control Engineering Practice*, 37:11–19, 2015. 23

APPENDIX A
DYNAMICAL BEHAVIOUR

A. Connection between object and robots

The connection between the robot and the object has influence on the dynamical behaviour of the system. Possible connections that are considered are, quasi-rigid, partially constrained and unconstrained. With the quasi-rigid connection, forces can be applied in all three degrees of freedom, but no movements are possible with respect to the object. A partially constrained connection makes it possible to apply force in one direction, both pushing and pulling. The movements with respect to the geometry are limited in the direction of the connection. Unconstrained connection, means that the robot can move with respect to the bed, but can only apply force in one direction by pushing the object. In order to determine which connection is preferred for the ROPOD project, there are multiple aspects that should be considered.

- To be able to handle different types of objects, the connection should be adjustable.
- The size of the combination of object and robots should be limited due to the limited operating space within hospitals, for example the combination should fit inside elevators or through doorways.
- The mass of the object will influence the amount of robots necessary to transport the object.
- The amount of force necessary to move the heavy objects and the limited amount of traction of the robot may result in the slipping of the robot. Additional force on top of the robot towards the floor may be needed in order to increase the traction, this additional down-force can be created by lifting the bed slightly.
- Omni-directionality is desired in order to maintain the manoeuvrability of the object.
- Fast breaking of the object should be possible at any time, due to operating in a not fully known environment.

Taking these aspects into account, having a quasi-rigid connection is preferred. With such a connection each robots can apply force to the object in the direction of the three degrees of freedom, thereby maintaining the omni-directionality of the object. Due to the ability to apply forces in all directions, the robots can be located at any position around the bed. While the other two connection methods need to have robots at all sides of the bed in order to maintain omni-directionality. However, depending on the design of the connection, it is less adjustable to different shaped objects in comparison to having no connection. With a fixed connection it is possible to lift the object, generating additional down-force on the robot, which has the result that the robot can exert more force without slipping. With the choice of a quasi-rigid connection between the robots and the object, the dynamics of the system are simulated with a three mass spring damper system.

B. State space representation of mass spring damper system

The mass spring damper system presented in Section III-A, is represented with the state space form (1). In order to analyse the dynamical behaviour of the plant, the system is first defined. The state $x(t)$ is defined as $x(t) = [x_1(t), x_2(t), x_3(t), \dot{x}_1(t), \dot{x}_2(t), \dot{x}_3(t)]$, where x_1 and x_3 are the position of the two robots and x_2 is the position of the object. The A matrix consists of the dynamics of the system, which is defined as

$$A = \begin{bmatrix} 0 & 0 & 0 & 1 & 0 & 0 \\ 0 & 0 & 0 & 0 & 1 & 0 \\ 0 & 0 & 0 & 0 & 0 & 1 \\ \frac{-k_1}{m_1} & \frac{k_1}{m_1} & 0 & \frac{-(d_1+c_1)}{m_1} & \frac{d_1}{m_1} & 0 \\ \frac{k_1}{m_2} & \frac{-(k_1+k_2)}{m_2} & \frac{k_2}{m_2} & \frac{d_1}{m_2} & \frac{-(d_1+d_2+c_2)}{m_2} & \frac{d_2}{m_2} \\ 0 & \frac{k_2}{m_3} & \frac{-k_2}{m_3} & 0 & \frac{d_2}{m_3} & \frac{-(d_2+c_3)}{m_3} \end{bmatrix} \tag{13}$$

Where k_i and d_i represent the stiffness of the i^{th} spring and damper respectively. The input $u(t)$ of the system is the forces applied by the two robots, therefore the B matrix is

$$B = \begin{bmatrix} 0 & 0 \\ 0 & 0 \\ 0 & 0 \\ \frac{1}{m_1} & 0 \\ 0 & 0 \\ 0 & \frac{1}{m_3} \end{bmatrix}. \tag{14}$$

The output of the system is defined as $y = [\dot{x}_1, \dot{x}_3]^\top$, which are the velocities of the two robots. The states of the object are not measured, therefore not visible in the output. Vectors C and D are

$$C = \begin{bmatrix} 0 & 0 & 0 & 1 & 0 & 0 \\ 0 & 0 & 0 & 0 & 0 & 1 \end{bmatrix} \tag{15}$$

$$D = \begin{bmatrix} 0 & 0 \\ 0 & 0 \end{bmatrix}. \tag{16}$$

The resulting state-space model is a linear, continuous, over-actuated multi-input-multi-output (MIMO) system. Which resembles the dynamical behaviour of the simplified system presented in Figure 3.

In order to determine the dynamical behaviour of the plant, a bode diagram is generated with the parameters presented in Table I, The mass and damping of the robots is set similar to

TABLE I
THE PARAMETERS OF THE SIMPLIFIED MASS SPRING DAMPER SYSTEM, USED FOR THE ANALYSIS OF THE PLANTS BEHAVIOUR.

Variable	Value	Unit
$m_{1,3}$	35.0	kg
m_2	100, 500	kg
$d_{1,2}$	0.01	Ns/m
$c_{1,3}$	5.00	Ns/m
c_2	10.0, 50.0	Ns/m
$k_{1,2}$	8.00×10^8	N/m

the mass and damping of the turtles, which are used for the experimental part, see Chapter VI. The mass of the object is varied between 100 and 500 kg in order to be similar to the hospital bed. The damping of the object is set to be equal to 10% of the mass. For simulation purposes, the parameters of

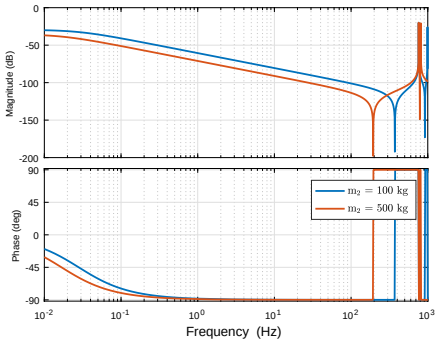

(a) Response of force input of robot 1 to velocity output of robot 1

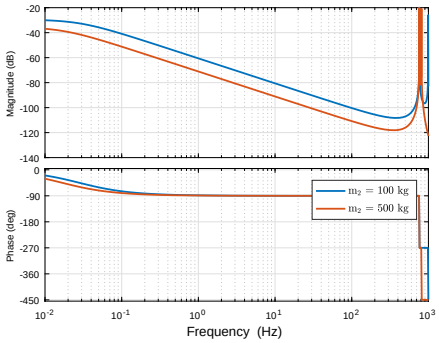

(b) Response of force input of robot 1 to velocity output of robot 2

Fig. 19. The bode plot of the simplified MIMO system.

the stiffness and damping of the connection are based on a connection with length L is 0.2 m and a surface area of A of 0.01 m^2.

The elastic modulus of aluminium is $E = 69 \times 10^9$ N/m^2 and the damping is $d_{1,2} = 0.01$ Ns/m [29]. Using,

$$k_{1,2} = \frac{EA}{L} \tag{17}$$

the stiffness of the connection is determined. The parameters of the connection influences the stiffness k_i, which influences the eigenfrequencies of the system. Therefore, the stiffness might influence the stability of the system, this is further investigated in Appendix D. In Figure 19, the bode of input of robot one to output of robot one and two are visualised. The bode diagram of input two to the output of robot one and two are the same since the two robots are similar. For a MIMO system, the input signal of input one effects the output of the second system, which is defined as the interaction of the system.

The physical effects of the system are visible in the bode diagram. The minus one slope for the frequencies between 10^{-1} and 10^1 Hz, is the mass of the system on velocity level. The zero slope for low frequencies is the effect of damping. There are four zeros present in the system and five poles, all poles are stable visible by their negative phase shift. The reason for the low magnitude of the entire system is the mass of the object, which is also visible by the comparing the effects of the change of m_2. The increase of m_2 from 100 to 500 kg decreased the magnitude of the system.

C. Range of the Inertia

The inertia of the object is dependent on both the dimensions as the mass of the object. Therefore, only an estimate of the inertia range can be provided. The inertia of the system is determined based on the simplified schematic drawing of the total system in Figure 20. The inertia of both the object as the robot is based on the inertia of a box shaped object with equally distributed mass, which is determined with,

$$I_{obj} = \frac{m_{obj}}{12}\left(l_{obj}^2 + w_{obj}^2\right) \tag{18}$$

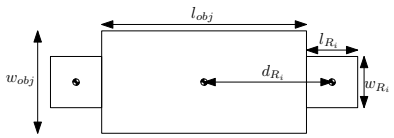

Fig. 20. Schematic diagram of system for the inertia determination.

where m is the mass, l is the length and w is the width. The inertia of the robots rotating around the centre of the object is calculated with,

$$I_{R_i} = \frac{m_{R_i}}{12}\left(l_{R_i}^2 + w_{R_i}^2\right) + m_{R_i} d_{R_i}^2. \tag{19}$$

The parameters of both the object and the robot are provided in Table II, which are based on the average bed size and the dimensions of the turtle.

TABLE II
THE PARAMETERS FOR THE ESTIMATED RANGE OF THE INERTIA OF THE TOTAL SYSTEM.

Variable	Value	Unit
m_{R_i}	35.0	kg
m_{obj}	100, 500	kg
l_{R_i}	0.50	m
l_{obj}	2.20	m
w_{R_i}	0.50	m
w_{obj}	1.00	m
d_{R_i}	$\frac{1}{2}(l_{R_i} + l_{obj})$	m

The distance d is the shift of the centre of mass of the robot to the centre of mass of the object. The inertia range for objects between 100 and 500 kg is between 115 and 310 kg·m^2. The range of inertia between an object mass of 100 kg and 500 kg, is dependent on the chosen dimensions of the real object and robot. However, the range is determined as an indication for the performance of the designed controllers in Section IV-A.

APPENDIX B
CENTRALIZED OR DECENTRALIZED CONTROL SCHEME

In case of the cooperative transportation both the centralized and decentralized structure is analysed. In order to compare the structures the state space representation of the mass spring damper system provided in Chapter III is controlled by the low level velocity controller designed in IV-A together with the feedforward controller. The communication between the two robots is simulated similar to the Zigbee network, with an interval of ± 10 Hz and a delay of 15 ms. Additional friction is implemented for a more close representation of the reality. First the centralized and decentralized control schemes are explained Section B-A and B-B. Thereafter, a preliminary comparison of performance is made Section B-C.

A. Centralized control scheme

A centralized control scheme, means that one central control unit (CCU) defines the necessary control signals for the system to follow the reference signal. One of the two robots functions as CCU robot which from now on is called robot one while the other robot is called robot two. The quasi-rigid connection between robot and object makes it able to estimate the velocity of the other robot. This will limit the influence of communication delays on the performance of the system. The velocity is necessary for the control of the system. Due to the communication delay, the control signal send from robot one to two is delayed as well. Therefore the control input from robot 1 is delayed with 15 ms. A schematic representation is provided in Figure 21.

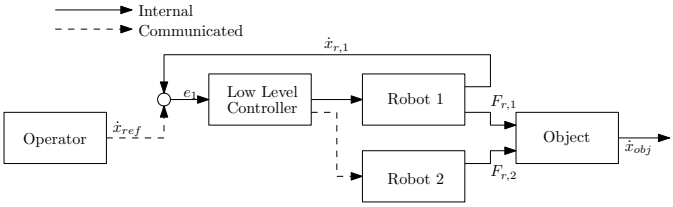

Fig. 21. Schematic diagram of centralized control plant

B. Decentralized control scheme

For the decentralized control scheme, the CCU is the operator which sends the reference signal to the individual robots. The low level controllers use the error between reference signal and the robots velocity as input signal. No additional communication is necessary among the two robots. The schematic representation of the system is visualised in Figure 22.

C. Preliminary Comparison of Performance

The performance of the two scheme is possible since they control the same system, with the same low level controller. The operator sends a direction command which is transformed to a reference signal for the individual robots via the transformation defined in C-A. The achieved velocities of the object

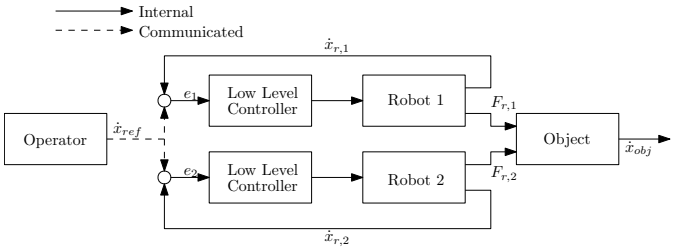

Fig. 22. Schematic diagram of decentralized control plant

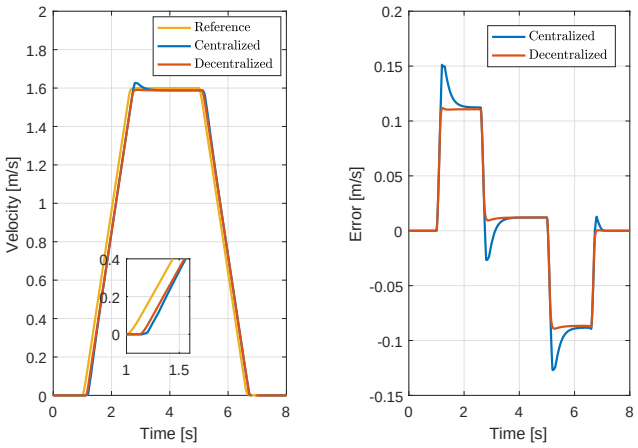

(a) The reference signal versus the objects velocities

(b) The error in velocities of the objects compared to reference signal.

Fig. 23. The performance of the centralized and decentralized control scheme

for both control schemes are shown in Figure 23a, and the corresponding error signal in Figure 23b.

The delay and interval of the communication between operator and robot results in a delayed response to the reference signal. For the centralized system, this delay is longer due to the additional communication between the two robots. The overshoot visible in Figure 23a, is caused by the interval of the communication, robot two is still applying force while robot 1 wants to compensate for the error. The effect of the delay and interval of the communication is clearly visible, if the input forces of the two systems are compared, Figure 24a.

The discretization of the input force signal for robot two due to the communication is the cause of the step like force applied by robot two. Another aspect that is less clear from the force input signals, is the internal force in the system, defined in Section III-C. During the reference signal, both system experiences internal force at 5.1s due to the shift in force direction. The magnitude of the internal force is where 4.2 and 0N, respectively the centralized and decentralized control scheme. The internal force of the centralized system is relatively small compared to the force applied on the system, however its magnitude increases if the communication interval or delay increases. If the delay is increased till 20 ms and the interval to 5 Hz, the internal force of the centralized system increases to 38.7 N. For the decentralized system, the internal

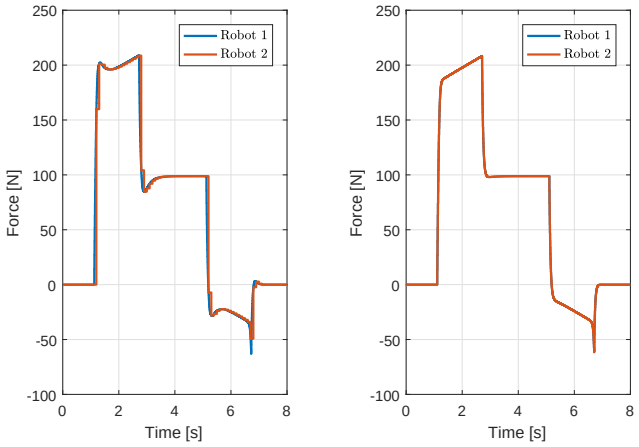

(a) Centralized (b) Decentralized

Fig. 24. The force inputs of the centralized and decentralized control scheme

force remains 0 N, however this is under the assumption that both robots obtain the reference at the same time.

Although the performance of the centralized and decentralized control schemes for this particular system are comparable. The centralized system is greatly depending on the communication between the two robots. If the communication interval, delay or package drop rate changes, the effects on the centralized system are greater compared to the decentralized system. And if the communication between the two robots fails, no movements are possible while the decentralized system can continue its movements. Therefore, the design structure of the cooperative transportation algorithm will be of a decentralized form.

APPENDIX C
HIGH LEVEL CONTROL

A. Reference Transformation

The signal obtained from the operator is defined as $\dot{q}_n$. The communication interval and delay as defined in Section III-B, are 10 Hz and 15 ms. Due to the difference in communication interval and operation frequency of 200 Hz, the obtained signal is discontinuous. The signal obtained of the operator is $\dot{q}_n \in \{\mathbb{R}^3, [-1, 1]\}$, resulting in a signal containing the desired direction and velocity of the object. This signal enters the Reference Transformation block together with the information of obstacle blockage o_b, see Figure 5. The Reference Transformation block is split into two sections, the transformation of $\dot{q}_n$ to a second order velocity reference signal $\dot{q}_{ref}$ and the transformation of the second order object reference to a robot reference signal $\dot{q}_{ref,i}$ according to (20).

A second order velocity reference signal means that there are bounds on the acceleration and jerk level. The first step is scale the reference signal $\dot{q}_n$ according to the maximum velocity v_{max}, which is defined by the system itself and set according to the requirements, see Section II-C. In order to apply constrains on acceleration level, the rate of increase and decrease of the signal is set to be equal to the limit of acceleration. A low pass filter of is used to limit the jerk to 6 m/s^3 in the reference signal $\dot{q}_{ref}$, for prove see Appendix C-C. The result of the transformation is the signal $\dot{q}_{ref,obj}$, an example is visible in Figure 25, with the belonging acceleration and jerk signal in Figure 26.

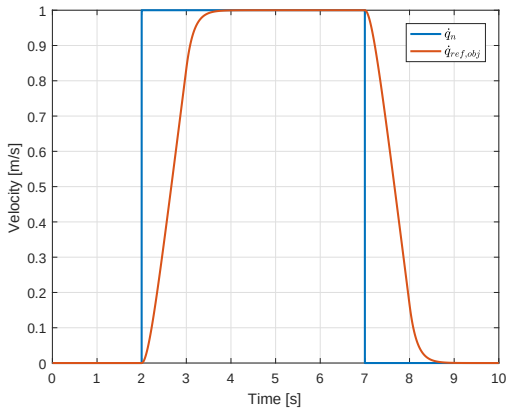

Fig. 25. The transformation from operator signal to object reference

The transformation from object reference to robot reference, results in a reference signal for each robot. When these reference signal is followed by the individual robots, the object will follow the object reference. The transformation is depending on the relative position $q_d = [x_{d,i}, y_{d,i}, \phi_{d,i}]^\top$ of the robot with respect to the object, see Figure 27. Due to the quasi-rigid link between robot and object, it is assumed that the value of q_d remains the same. The resulting transformation

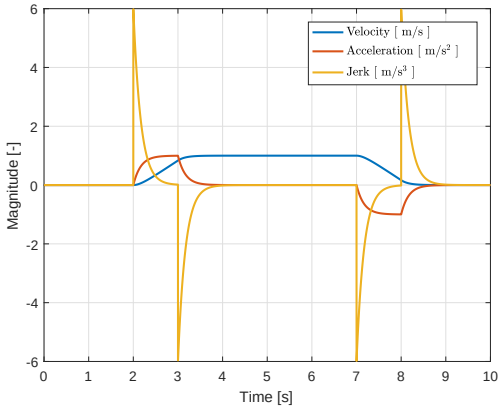

Fig. 26. The acceleration and jerk of the reference signal.

is achieved by:

$$\begin{bmatrix} \dot{x}_{ref,i} \\ \dot{y}_{ref,i} \\ \dot{\phi}_{ref,i} \end{bmatrix} = \begin{bmatrix} \dot{x}_o \\ \dot{y}_o \\ \dot{\phi}_o \end{bmatrix} + \dot{\phi}_o \begin{bmatrix} x_{d,i} \\ y_{d,i} \\ 0 \end{bmatrix} \tag{20}$$

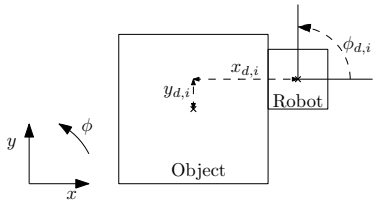

Fig. 27. The definition of the relative position of the robot with respect to the object

The final step within the reference transformation, is the adjustment of the reference signal in case of obstacle blockage. The signal received from the obstacle collision detection o_b is either zero or one, in case the signal is one a obstacle is blocking the current reference path. While o_b is equal to one, the reference signal $\dot{q}_n$ is set to zero for all directions.

B. Obstacle Collision Detection

Obstacles are a major issue in the surroundings of autonomous robots, although the cooperative transportation of objects will not be done autonomously, the robots should prevent collisions with obstacles. The goal of the obstacle collision avoidance is not to steer around the obstacles that blocks the path of the robots. The large dimensions and mass of the object make any unexpected movements, like moving around an obstacle, a risk for its surroundings. In order to detect an obstacle in the world around the robot, it is assumed that the robot has a method where its relative distance and angle to the obstacle is measured. For obtaining this data, a laser range finder or a self generated world model can be used. With this knowledge and the knowledge of the dimensions of the obstacle, the robot needs to decide whether its current

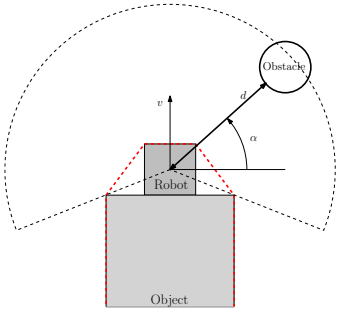

Fig. 28. Simplification of the world model of the robot

path is blocked by the obstacle. A simplification of the world model, known to the robot is visualised in Figure 28.

Half of the entire system is shown, one robot and half of the object. In the world model, the visibility range is defined as the black dotted line, within this range the robot is able to detect the obstacle. The velocity reference v is depicted as the black arrow, the convex body where within the obstacle is not allowed, is visualised with the red dotted line. Once an obstacle enters the visibility field of the robot, the relative distance d and angle α is determined. The next step is determining the closest point on its convex body with respect to the obstacle. The evolution over time of the system is based on the reference signal received from the operator at the current time, see Figure 29. In order to determine the time horizon of the prediction, the maximum time for deceleration to stand still needs te be determined, which is depending on the maximum velocity v_{max}, acceleration a_{max} and a safety ratio. So for a $v_{max} = 1.6$ m/s and $a_{max} = 1$ the minimal time of deceleration is 1.6 second, with additional safety this is increased till 2.5 second. With a frequency of 200 Hz the robot estimates its position during a 2.5 seconds time window. Every time step of 0.1 second within this 2.5 seconds window, the closest distance between obstacle and convex body is determined. Based on this relative distance, the robot predicts if it or the object is going to collide with the obstacle, based on its current reference velocity. In the next section, the steps that are taken once an obstacle is blocking the path are defined.

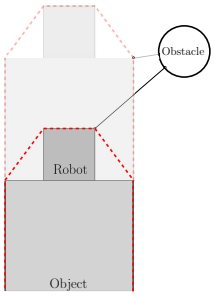

Fig. 29. Shortest distance to convex body and its time evolution

If the obstacle is not blocking its estimated path, the robot will continue its current trajectory. Otherwise it brakes in order to prevent collisions and sets its reference signal at zero as long as its estimated path is blocked. If the reference signal is changed, a new path is estimated and the process is repeated. The adjustment of the reference signal happens before the velocity transformation defined in Section C-A, hence the breaking of the system is not sudden, but happens according to bounded acceleration and jerk reference signal. However, this increases the response time to sudden obstacles. Sudden obstacle blockage will need a different safety measure.

C. Acceleration and Jerk Limiter

The jerk is the second derivative of the velocity reference signal. The limitation of the jerk of the reference signal is important for the comfort of the patient. The reference signal obtained of the operator is $\dot{q}_n \in \{\mathbb{N}^3, [-1, 1]\}$, which is a step function. Using a rate limiter, which determines the derivative of signal with

$$rate(i) = \frac{u(i) - q_r(i-1)}{t(i) - t(i-1)} \tag{21}$$

where $u(i)$ is the current input at time $t(i)$, and $q_r(i-1)$ is the previous output at time $t(i-1)$. Depending on this derivative, the output of the rate limiter q_r is determined. If the derivative is greater than the maximal admissible acceleration a_{max}, then $q_r(i) = Tsa_{max} + q_r(i-1)$, where Ts is the sample time. However, if the derivative is smaller, the output is $q_r(i) = u(i)$. This limits the acceleration of the reference signal.

The jerk limitation is achieved with a low pass filter, with the form,

$$T(s) = \frac{z}{s+z} \tag{22}$$

where s is the Laplace operator and z is the jerk limit. In order to state that the low-pass filter limits the jerk, the situation with the highest jerk is analysed. The highest jerk is present within the reference signal, if the system switches from negative acceleration $-a_{max}$ to positive acceleration a_{max}. This situation is comparable to a step function at $t = 0$ with amplitude $2a_{max}$. Therefore,

$$\dot{q}_a(t) = \begin{cases} 2a_{max}, & t \geq 0 \\ 0, & t < 0, \end{cases} \tag{23}$$

where $\dot{q}_a(t)$ is the derivative of the velocity reference $q_a(t)$. Taking the Laplace transform of the signal of $\dot{q}_a(t)$,

$$\mathcal{L}\{\dot{q}_a(t)\} = s\mathcal{Q}(s) = \frac{2a_{max}}{s}. \tag{24}$$

Due to the fact that the derivative of the signal $q_a(t)$ is used, the $s\mathcal{Q}(s)$ is integrated in order to obtain the Laplace transform of q_a,

$$\mathcal{Q}(s) = \frac{2a_{max}}{s^2}. \tag{25}$$

The obtained signal is multiplied by the low pass filter (22),

$$T(s)\mathcal{Q}(s) = \frac{2a_{max}z}{s^2(s+z)}. \tag{26}$$

The result is the Laplace transform of the output signal of the low pass filter and therefore equal to the reference signal

for the object $q_{ref,obj}$. In order to investigate the limit on the jerk of the signal $q_{ref,obj}$ the second derivative of the signal is taken $\ddot{q}_{obj,ref}$,

$$\mathcal{L}\{\ddot{q}_{ref,obj}(t)\} = s^2\mathcal{Q}_{ref,obj}(s) = \frac{2a_{max}z}{s+z}. \tag{27}$$

According to the initial value theorem presented in [30], the maximum value of the signal $\ddot{q}_{ref,obj}(t)$ at $t = 0$ can be obtained. Using

$$\begin{aligned}\ddot{q}_{ref,obj}(0) &= \lim_{s\to\infty} s\left(s^2\mathcal{Q}_{ref,obj}\right) \\ &= \lim_{s\to\infty} \frac{2a_{max}zs}{s+z} \to 2a_{max}z. \end{aligned} \tag{28}$$

the initial value is determined, which is equal to the step size of the jerk at $t = 0$. Furthermore, the final value of the signal can be determined using the final value theorem presented in [30].

$$\begin{aligned}\ddot{q}_{ref,obj}(\infty) &= \lim_{s\to 0} s\left(s^2\mathcal{Q}_{o}\right) \\ &= \lim_{s\to 0} \frac{2a_{max}zs}{s+z} \to 0. \end{aligned} \tag{29}$$

Therefore, it can be stated that the maximum jerk value is equal to $2a_{max}z$. The value of the low pass filter z, is set according to $z = \frac{j_{max}}{2a_{max}}$, where j_{max} is the jerk limited prescribed by the requirements.

APPENDIX D
STABILITY ANALYSIS

The system is a multi-input-multi-output system (MIMO), for the three dimensional case six inputs and six outputs. The controllers presented in Chapter IV, result in a stable system if the interaction between the robot's input and the output of the other robot is neglected. However, these interaction forces may result in an unstable system. Therefore, the stability of a one dimensional MIMO system is investigated to determine the impact of the quasi-rigid connection. Furthermore, due to the fact that the system has three degrees of freedom, the stability of the three dimensional MIMO system is also investigated.

A. One Dimensional MIMO system

The one dimensional MIMO system stability analysis is performed in order to guarantee the stability of using multi robots which are quasi-rigid connected. The system can be simplified to the schematic representation depicted in Figure 30.

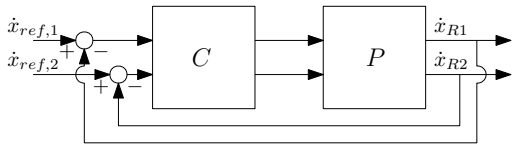

Fig. 30. Schematic representation of a one dimensional MIMO system, where K is a diagonal controller with on the diagonal the controller $C_{fb,xy}$. The plant P, is the mass-spring-damper system presented in Section III, where the dynamics of the robot is the FRD of the turtle.

Due to quasi-rigid connection between the robot and the object, the input of one robot effects the output of the other robot. Therefore, the factorized Nyquist test presented in Section V-C is used for the stability analysis. The result of the two tests is visible in Figure 31, where the stability is analysed for the system with object masses 100 and 500 kg and the parameters of the connection presented in Table I. For the analysis the FRD of the robots is used to have a close resemblance of the real system. The SSV of both systems are comparable for the low frequencies therefore only one is displayed. From Figure 31a it can be concluded the first criteria is satisfied, the diagonal system $\tilde{P}$ does not make an encirclement of the origin. The second criteria based on the SSV is satisfied because $\bar{\sigma}(\tilde{T})$ for both object masses remains below the SSV of E, see Figure 31b. Therefore it can be concluded that the one-dimensional MIMO system is stable with the provided controller $C_{fb,xy}$ and the object masses of 100 to 500 kg.

The value of the stiffness was set to be equal to a value based on an example connection, however the real stiffness of the connection is unknown. Hence an analysis is performed in order to determine the influence of the stiffness on the stability of the system. The factorized Nyquist test, using (11), is used to investigate the stability. For systems with the stiffness higher than 10^7 N/m, the stability of the MIMO system can be guaranteed.

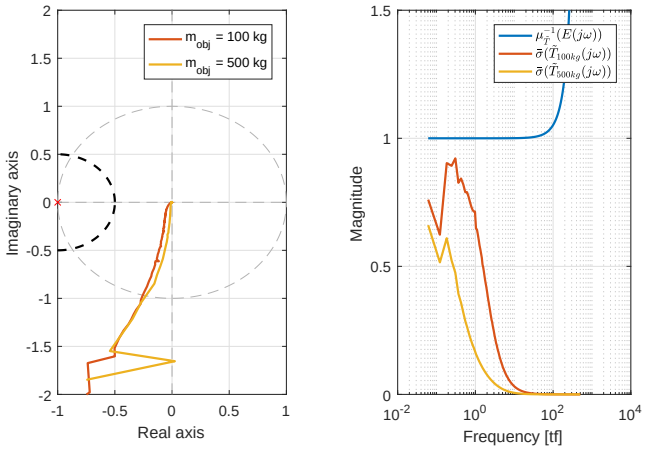

(a) The nyquist plot of the open-loop MIMO diagonal system for two masses.

(b) The comparison of the maximum singular value of $\tilde{T}$ with respect to the structured singular value of E.

Fig. 31. The two criteria of the factorized Nyquist test, in order to guarantee stability of the one dimensional MIMO system.

The next stability analysis is based on the three dimensional MIMO system.

B. Three Dimensional MIMO System

For the three dimensional case, the system is simplified. The reason for the simplification is the fact that, as defined in Section III, the low frequent dynamics of the system is comparable to a simple mass-damper system. Assuming a perfect quasi-rigid connection, the dynamics of the system can be modelled by a single mass-damper. Therefore, the three dimensional case is consisting only of a mass-damper, where the mass and damping constants are of the object and robots together. The structure of the system is depicted in Figure 32.

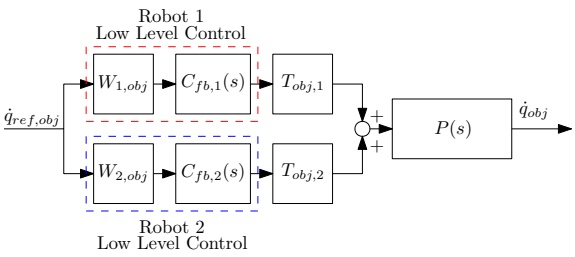

Fig. 32. Schematic representation of the three dimensional MIMO system, which is simplified to a mass-damper system where the low level control of the robots is controlling the system. The reference signal is first transformed using $W_{i,obj}$, as defined in (20), to the position of the robots. After which the feedback controller generates the forces necessary for the movement, these forces are transformed to the position of the centre of the object, using $T_{obj,i}$ as defined in (9). The combined forces of robot 1 and 2 are applied on the mass damper system.

The input of the open-loop system is the reference signal for the object, each robot transforms this signal using (20) to the reference signal for the robots. The feedback controllers designed in Section IV-A generate the force which is transformed to the centre of mass of the bed using the transformation

presented in Section V-A. The resulting system is a three dimensional representation of the real system, where there is no interaction between the three inputs and outputs of the system. Therefore, the stability analysis can be performed on individual inputs using the single-input-single-output (SISO) stability check. The SISO stability check is based on the eigenvalues of the system and the encirclements of the minus one point in the Nyquist plot. Using the parameters presented in Table III

TABLE III
THE PARAMETERS OF THREE DIMENSIONAL SYSTEM, USED FOR THE STABILITY ANALYSIS.

Variable	Value	Unit
$m_{x,y}$	$170 - 570$	kg
I_z	$115 - 310$	mL^2
$d_{x,y}$	17.0	Ns/m
d_z	11.5	Ns/rad
$L_{y,1}$	1.00	m
$L_{y,2}$	-1.00	m
l_{obj}	2.00	m
w_{obj}	1.00	m

The inertia I_z is based on estimation of the inertia in Appendix A-C. The resulting three dimensional open-loop system contains only poles and zeros in the left half plain, therefore the resulting Nyquist plot of the system must not contain an encirclement of the minus one point in order to prove the stability of the system with the provided parameters. In Figure 33a, the resulting Nyquist diagram is visible where it is clear that the minus one point is not encircled and it can therefore be concluded that the three dimensional system is stable for the given parameters. The inertia scales quadratically based on the dimensions of the object, therefore, the number used is based on the average dimensions of hospital beds and the lowest mass. Therefore, the inertia in Table III is assumed to be the lowest bound of the inertia, guaranteeing the stability of the lowest bound will proof to be guaranteeing the stability of any inertia higher that this mass, see Figure 33b. However, the performance will drastically drop with increasing inertia.

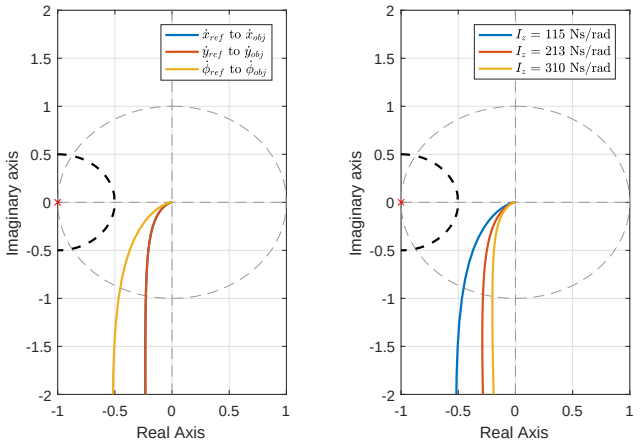

(a) The Nyquist diagram of the three dimensional system. The contour of the x-axis is directly under the contour of the y-axis. The contour does not make any encirclements of the -1 point and is therefore guaranteed stable.

(b) The influence of the inertia of the system, it is clear that the lowest inertia, determined in Appendix A-C, is stable. Increasing the inertia will not result in instability, however it will result in decrease in performance.

Fig. 33. The Nyquist diagram of the three dimensional system and the influence of the inertia of the system.

APPENDIX E
PARAMETER ESTIMATION

In order to have an estimation of the systems parameters for the tuning of both the feedforward as the observer, these parameters should be estimated every time the load between the robots changes. Estimating these parameters based on a simple motion or during the performance of tasks is desired. A method where a simple motion is used for the estimation of the parameters of the system is presented in [31]. The iterative motion feedforward tuning presented in this paper, uses a polynomial parametrized feedforward which parameters represent physical aspects of the system, therefore, it is a possible method to be used to obtain the mass and inertia of the system. First a short description of the method is given after which the initial results are presented. The method is not experimentally verified for the reason that the estimation is not part of the research, the theory presented is merely given as example.

A. Theory

The system that is analysed is a discrete-time, single-input-single-output and linear time-invariant system, defined as $P(q)$, where q denotes the forward shift parameter. $C_{fb}(q)$ and $C_{ff}(q)$ represent respectively the feedback and feedforward controller. r is the reference signal and v the disturbance caused by sensor noise. The schematic overview is visualised in Figure 34.

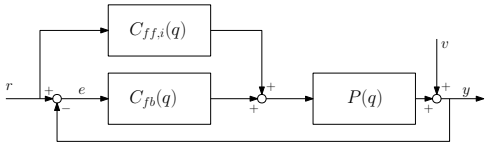

Fig. 34. Schematic plant representation

The parameters that are used within the feedforward $C_{ff}(q)$ are compensating for the effects of acceleration, jerk and snap. Meaning that the mass of the system can be obtained using the proposed method. Using a simple point to point motion, where the system starts in rest and ends in a rest position, the systems behaviour is determined. A minimizing quadratic function based on the error e and output signal y, where the error signal is defined as $e = r - y$. the parameters of the feedforward are adjusted. For a more elaborate explanation and proof see [31].

B. Simulation results

The mass spring damper system presented in Section III-A is used as plant model. Although the system is MIMO, it is assumed that the inputs that are applied by each robot are the same, which is the case for the centralized controller in a 1 dimensional problem. The output of the system is no longer the velocities of the two masses which represent the robots, but the velocity of the object mass that is transported. The resulting system is a discrete-time, SISO system with a friction model consisting of damping. The resulting state space representation is given by (1). Where,

$$A = \begin{bmatrix} 0 & 0 & 0 & 1 & 0 & 0 \\ 0 & 0 & 0 & 0 & 1 & 0 \\ 0 & 0 & 0 & 0 & 0 & 1 \\ \frac{-k_1}{m_1} & \frac{k_1}{m_1} & 0 & \frac{-d_1}{m_1} & \frac{d_1}{m_1} & 0 \\ \frac{k_1}{m_2} & \frac{-(k_1+k_2)}{m_2} & \frac{k_2}{m_2} & \frac{d_1}{m_2} & \frac{-(d_1+d_2)}{m_2} & \frac{d_2}{m_2} \\ 0 & \frac{k_2}{m_3} & \frac{-k_2}{m_3} & 0 & \frac{d_2}{m_3} & \frac{-d_2}{m_3} \end{bmatrix},$$

$$B = \begin{bmatrix} 0 \\ 0 \\ 0 \\ \frac{1}{m_1} \\ 0 \\ \frac{1}{m_2} \end{bmatrix}, C = \begin{bmatrix} 0 & 0 & 0 & 0 & 1 & 0 \end{bmatrix}, D = \begin{bmatrix} 0 \end{bmatrix}. \quad (30)$$

The controller $C_{fb}(q)$ that is used during the parameters estimation is presented in Chapter IV. The feedforward controller $C_{ff,i}(q)$ is simplified in comparison to the one presented in Chapter IV, for the reason that only the mass is estimated, the indices i represents the iteration. Therefore, the feedforward controller is only consisting of

$$C_{ff,i}(q) = \frac{q^2 - 2q + 1}{T_s^2 q^2} \theta_{acc,i}. \quad (31)$$

Where T_s is the sample frequency and $\theta_{acc,i}$ is the estimated mass of the system at the i^{th} iteration. The parameters of the system are as defined in Chapter III, for the initial estimate of the mass $\theta_{acc,1} = 180$ kg. There is no static and dynamic friction included in the system, for the reason that the algorithm is unable to estimate the mass if these friction components are present in the system. However, if the friction coefficients are compensated by the feedforward, the estimation is possible. Noise is entered in to the system as v, see Figure 34. A third order reference signal is used, like the one presented in Figure 35, in order to obtain the error caused by the initial mass error. Based on the obtained error and the output signal of the system, the adjustment of $\theta_{acc,1}$ is determined using the equations presented in [31]. The resulting estimated mass is $\theta_{acc,2} = 201.2$ kg, which is a close approximation of the mass based on a single motion. More iteration can be performed, as long as the data that is analysed satisfies the conditions mentioned in Section E-A.

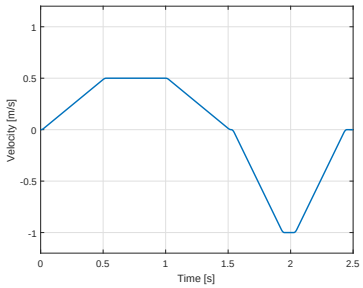

Fig. 35. Third order reference signal on velocity level

APPENDIX F
EXPERIMENTAL PERFORMANCE COMMUNICATIVE SYSTEM

A. Low Level Controller Performance

The performance of the communicative system is analysed, initially the impact of the feedforward controller after which the performances in the three degrees of freedom. The feedback controllers that are applied on the each robot in are defined in Section IV-A. The performance of the x and ϕ direction is only determined for the system with feedforward controller active. The reference signal sent to the robots is of the form prescribed in Section C-A. The reference signal applied on the system is a five seconds movement with 1 m/s velocity. The resulting reference tracking is visible in Figure 36a, the belonging filtered error signal in all three degrees of freedom are visible in Figure 36b. The error of the movement

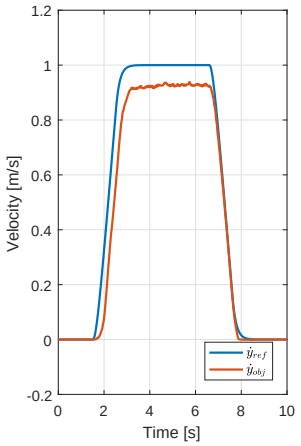

(a) The reference tracking.

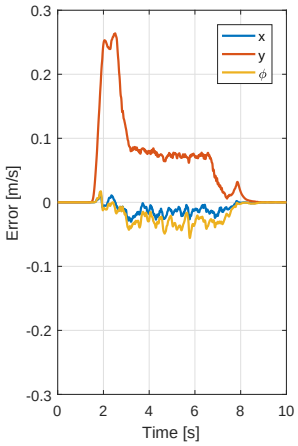

(b) the error signal in all three directions.

Fig. 36. The reference tracking in y direction of the communicative system without feedforward controller, where the resulting velocity $\dot{y}_obj$ is the estimated velocity of the object based on the velocity of the robot.

in y direction is constant during constant velocity, which is caused by the damping of the system. This effect is already noticed during the design of the controller in Section IV-A. The maximum error is not within the error margin set for the design of the feedback controller, however the error during constant motion is well within the criteria. The next step is including the feedforward controller, designed in Section IV-A. The results are visible in Figure 38.

The constant error during constant velocity is diminished from 0.17 to 0.06 m/s, which can be further diminished if the estimated parameters of the object are improved. The response time of the system is increased, due the fact that the feedforward has no phase lack in comparison with the feedback controller. The initial error still present in the system is caused by the static friction, which is not compensated in with the feedforward controller. However, the overall performance is within the design criteria specified. The performance in x

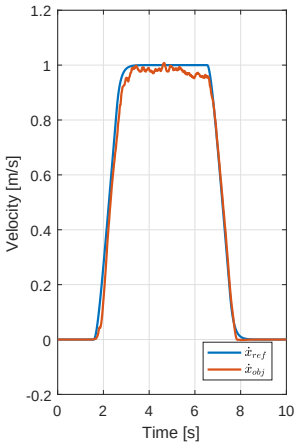

(a) The reference tracking.

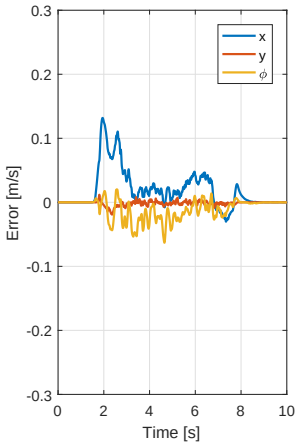

(b) the error signal in all three directions.

Fig. 37. The reference tracking in x direction of the communicative system with feedforward controller, where the resulting velocity $\dot{x}_{obj}$ is the estimated velocity of the object based on the velocity of the robot.

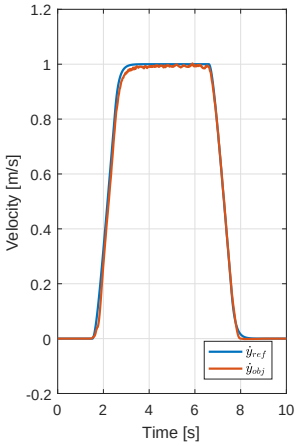

(a) The reference tracking

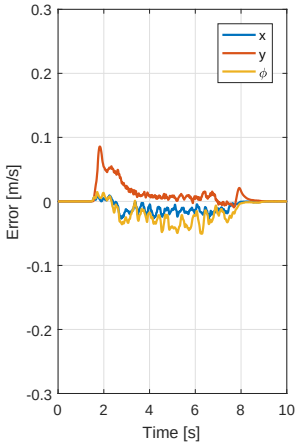

(b) the error signal in all three directions.

Fig. 38. The reference tracking in y direction of the communicative system with feedforward controller, where the resulting velocity $\dot{y}_{obj}$ is the estimated velocity of the object based on the velocity of the robot.

and ϕ direction of the bed are visible in Figures 37 and 39 respectively.

From the resulting performance of the three degrees of freedom it can be concluded that the system accurately follows the system with a maximum error of 0.10 m/s and 0.17 rad/s for the rotation. Although that the velocity signal is filtered with a low pass filter at 1 Hz, the resulting motion in x and y direction is smooth, without high acceleration shifts. The rotational movement, has a overshoot of the rotation velocity, however, the constant overshoot is well within the specified bound of 15%, prescribed by the controller design. The drift in x, y and ϕ noticeable in the error signal of all three

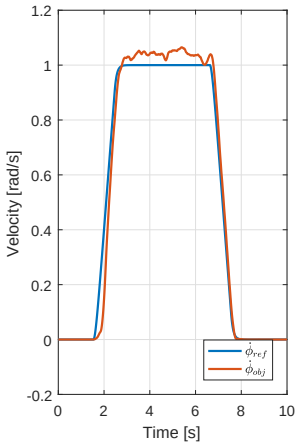

(a) The reference tracking.

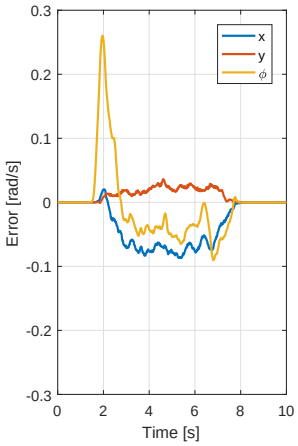

(b) the error signal in all three directions.

Fig. 39. The reference tracking in x direction of the communicative system with feedforward controller, where the resulting velocity $\dot{\phi}_{obj}$ is the estimated velocity of the object based on the velocity of the robot.

movements, is mainly caused by the error in the estimation of the relative position of the robot with respect to the bed.